Deuterium Fusion Using

Inertial Electrostatic Confinement (IEC)

February 2012

Contents

A. Introduction

a. Background Information

Nuclear fusion is a reaction involving the merging of nuclei of two atoms of sufficient energy. The result of the reaction is a single atom of a different element and one or more subatomic particles such as protons and neutrons. Fusion is intriguing to science because of the potential for harnessing the energy released from the reactions, but even though fusion is common in the universe, it is a difficult reaction to control. Recent fusion research has focused on large-scale efforts such as the Tokomak reactor, which uses magnetic confinement to induce super heated plasma to simulate the conditions of a star. These efforts have produced fusion, but at a large financial cost, and the reactions have not had practical use.

Other methods are known to produce fusion conditions. Examples include sonofusion, which involves inducing super hot temperatures on the surfaces of a bubble in a liquid with sonic pulses. This reaction is also known as bubble fusion, but so far, the concept has produced almost immeasurable results (Putterman).

Another method is Inertial Electrostatic Confinement (IEC). IEC uses electrical fields to force the acceleration and collision of charged particles. With sufficient voltages and fuel elements, IEC has been shown to produce fusion. This method was theorized by Elmore, Tuck, and Watson in the late 1950's, and Philo

Farnsworth, the inventor of television, demonstrated a device soon after. Hirsch and Farnsworth ultimately patented a device (Donovan).

IEC fusion did not receive as much research attention as magnetic confinement because it was not believed that large-scale power reactors could be made using IEC. More recently, IEC research has shown that it has the potential to be more obtainable as a useful fusion reaction than all other known methods. Beyond energy, an IEC device can be a practical source of neutrons for research and testing. For example, neutron fluxes are useful for radiographic imaging because the penetrating characteristics of neutrons allow passage through heavier atoms and collisions with lighter ones resulting in an alternate to traditional x-ray imaging. Other uses of neutrons include weapons detection through nitrate backscatter, neutron activation analysis, and medical isotope production (Donovan). Currently, neutron fluxes for these purposes are created with fission reactors or intensely radioactive transuranic isotopes. Reactors and radioactive material have inherent hazards, but IEC reactors do not have residual radioactive material or energy (Kulcinski). The fusion stops as soon as the reaction conditions are interrupted. Additionally, the scale of an IEC device is not limited by large amounts of shielding or critical masses of difficult to obtain material. IEC fusion can be achieved with a variety of materials including isotopes of hydrogen such as deuterium and tritium (Donovan). Deuterium is naturally occurring, and tritium is a byproduct of fission reactors. IEC devices are also

portable. The lack of size scale limitations enhances the possibility of practical applications.

b. IEC Theory

IEC fusion involves establishing a strong electrical potential well in the center of two concentric spheres, and fuel atoms are allowed to freely travel within both spheres (Ligon). The outer sphere is an anode with a positive charge. The inner sphere is a highly transparent cathode with a negative charge. The relative transparency of the inner sphere or grid allows charged particles accelerating toward it to become confined within it with minimal collisions with the inner grid.

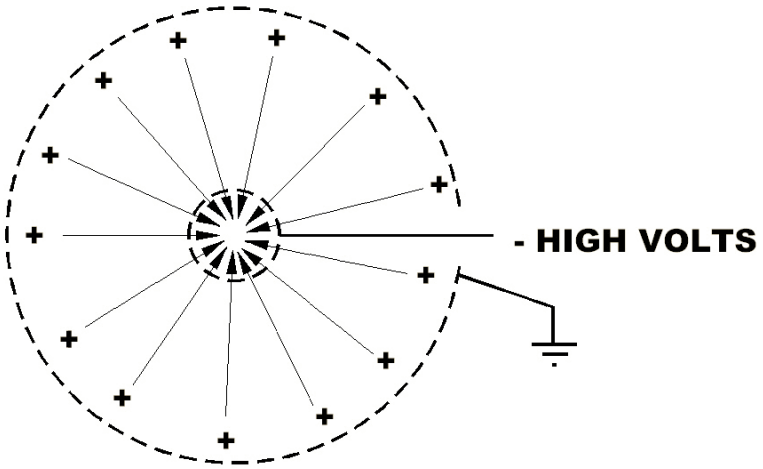

Figure 1: Basic schematic of an IEC device showing positive ions drawn to confinement inside a negatively charged inner grid (Ligon).

In order for the positively charge ions, or fuel, to have sufficient energy to fuse, they should only collide with other fusion fuel and only after being accelerated. This means that the IEC grids should not be densely packed with atoms and should not be contaminated with non-fuel ions. This is achieved by reducing the pressure in the device to sub-atmospheric pressures.

The fuel atoms become ionized to start the reaction through acceleration of naturally occurring ions. These occur naturally through reactions with cosmic radiation. The remaining fuel atoms become ionized through interaction with the starting ions through a concept known as Paschen discharge. A Paschen discharge occurs when specific voltage, acceleration length, and space between atoms, exist (Ligon).

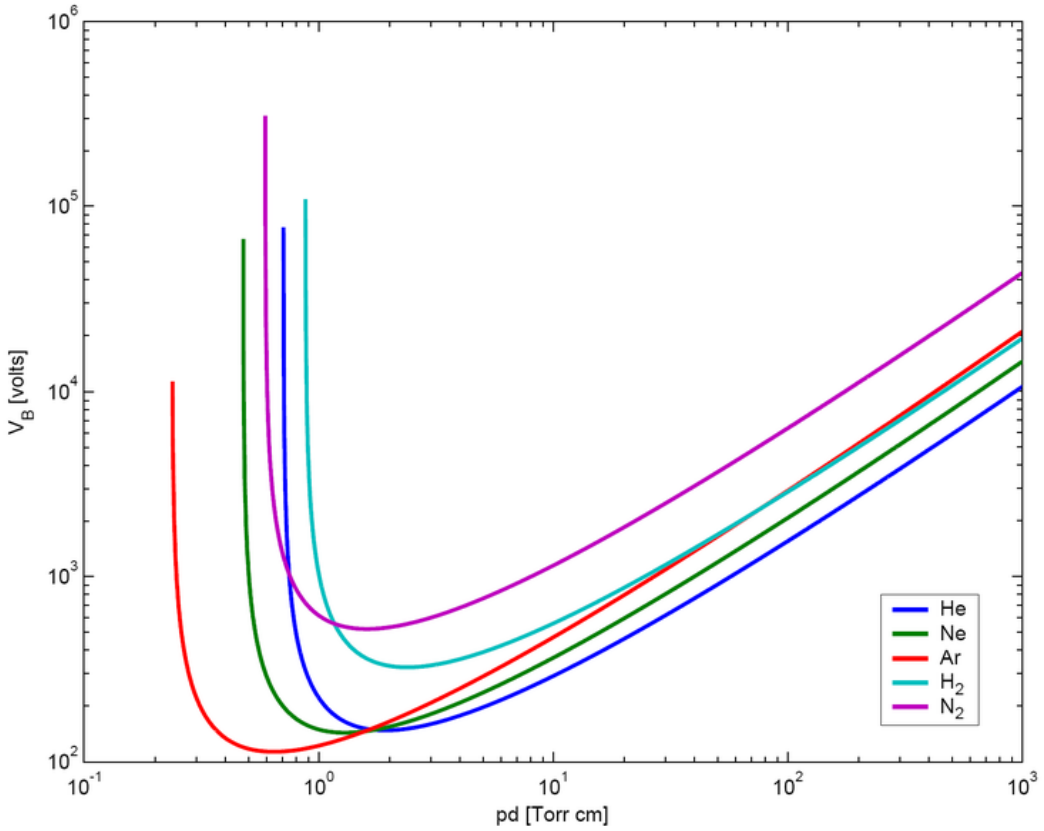

Figure 2: Paschen curve for several common elements. IEC is normally in the steep, left hand side of the curve. The voltage required to cause a discharge varies with atomic density expressed by pressure in Torr and the relative distance between the grids in cm (Wikipedia).

A Paschen discharge results in plasma of positively charged fuel ions. When confined, the plasma temperature can reach hundreds of millions Kelvin (Donovan). Sustaining the plasma gives a sustained chain of fusions.

A common fusion fuel is deuterium, which is a naturally occurring isotope of hydrogen whose nucleus contains one proton and one neutron. Two deuterium atoms can be fused together in an IEC device with the following possible reactions:

- ${}_{1}^{2}D + {}_{1}^{2}D \rightarrow {}_{0}^{1}n$ 2.5 MeV + ${}_{2}^{3}He$ (yield is one neutron, an isotope of helium,)
- ${}_{1}^{2}D + {}_{1}^{2}D \rightarrow {}_{1}^{1}p$ 3.0 MeV + ${}_{1}^{3}T$ (yield is one proton, tritium,)

These two reactions occur with an approximate 50 percent likelihood for each (Hull).

Fusion involving other isotopes is possible, but for this project, deuterium was examined because it can be legally owned without a license.

c. Hypothesis and Project Goals

This project had a dual purpose. The first purpose was to design and construct an IEC fusion device using commonly available materials to demonstrate the obtainability of fusion with the IEC concept.

The second goal was to build a device that could be used for future research and testing that makes use of fusion byproducts such as neutrons.

It was expected that by performing this project, the following scientific and engineering areas would be studied for learning:

- Nuclear physics and radiochemistry
- Radiation and neutron detection
- Mechanical engineering
- Electrical engineering

- Electrical and pressure instrumentation concepts
- Radiation protection
- Vacuum technology
- Material science
- Regulatory adherence

B. Materials

The design and assembly of the IEC device represented the bulk of the work of this project. The theoretical concepts of IEC fusion were incorporated into the design along with consideration of personnel safety and availability of parts. The device was an assembly of different parts and systems that can be described separately.

a. Fusion Fuel

Deuterium makes a good fusion fuel because is easily obtained and because it has a cross section for fusion reactions that makes it obtainable within an IEC plasma (UK).

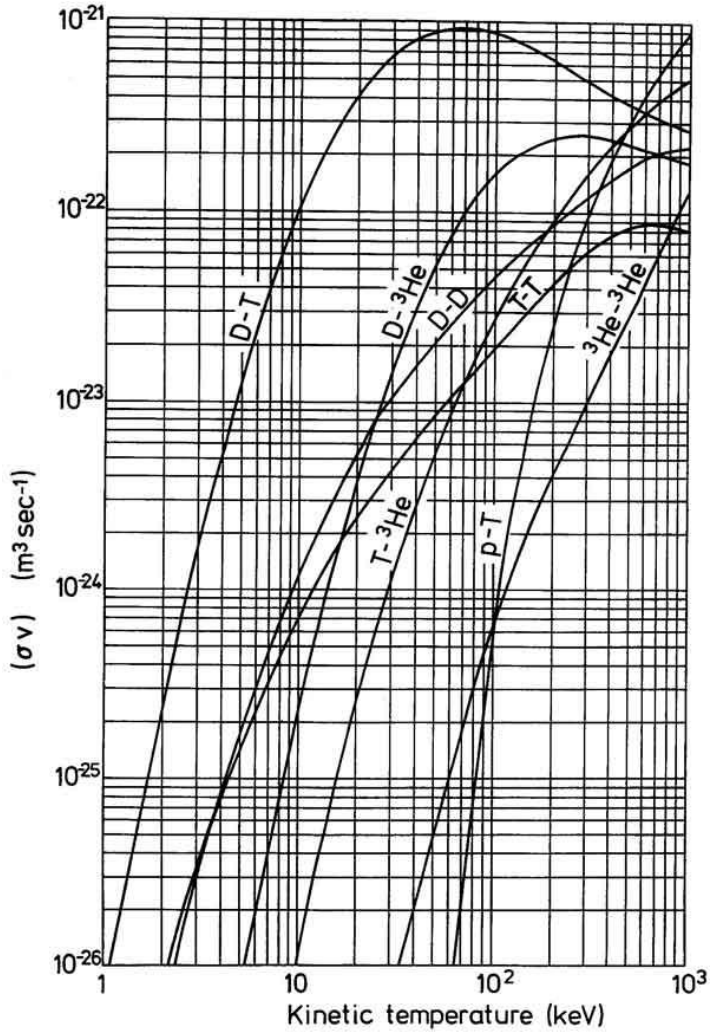

Figure 3 – Fusion reaction cross sections for various deuterium fusions including fusion with deuterium and an isotope of helium (UK).

The curves above show that D-D fusion reaction rates increase with temperatures expected for IEC plasma.

Deuterium can be found in nature as a small fraction of all hydrogen. Deuterium is extracted for various purposes including use of heavy water in some nuclear reactors and for chemistry research as a tracer. Deuterium is available as a pure

gas or as part of a molecule like heavy water, D2O. For this project, gaseous deuterium was ideal because it can be added in very small quantities as needed to control the fusion reaction. In a pure gas form, no other processing would be needed.

The United States Nuclear Regulatory Commission does regulate the sale of deuterium (USNRC). This limitation is needed because deuterium can be used in fission reactors and therefore in the production of atomic weapons. The regulations impose limits on the export of deuterium, but it is legal for a United States citizen to own.

Fusion does not require large amounts of deuterium. A small, pressurized lecture bottle contains enough gas for small-scale fusion devices, and a bottle containing 1850 psig was obtained from a gas supply company (see Figure 4).

Deuterium gas is hazardous because, like all hydrogen, it is flammable. Normal industrial safety practices for handling pressurized gases were followed, and the gas supplier provided a Material Safety Data Sheet (Tri-Gas).

In order to inject the deuterium fuel, a regulator was needed to reduce the bottle pressure. A needle valve was used for even finer control of the deuterium flow. Stainless steel tubing was used to keep the fuel pure.

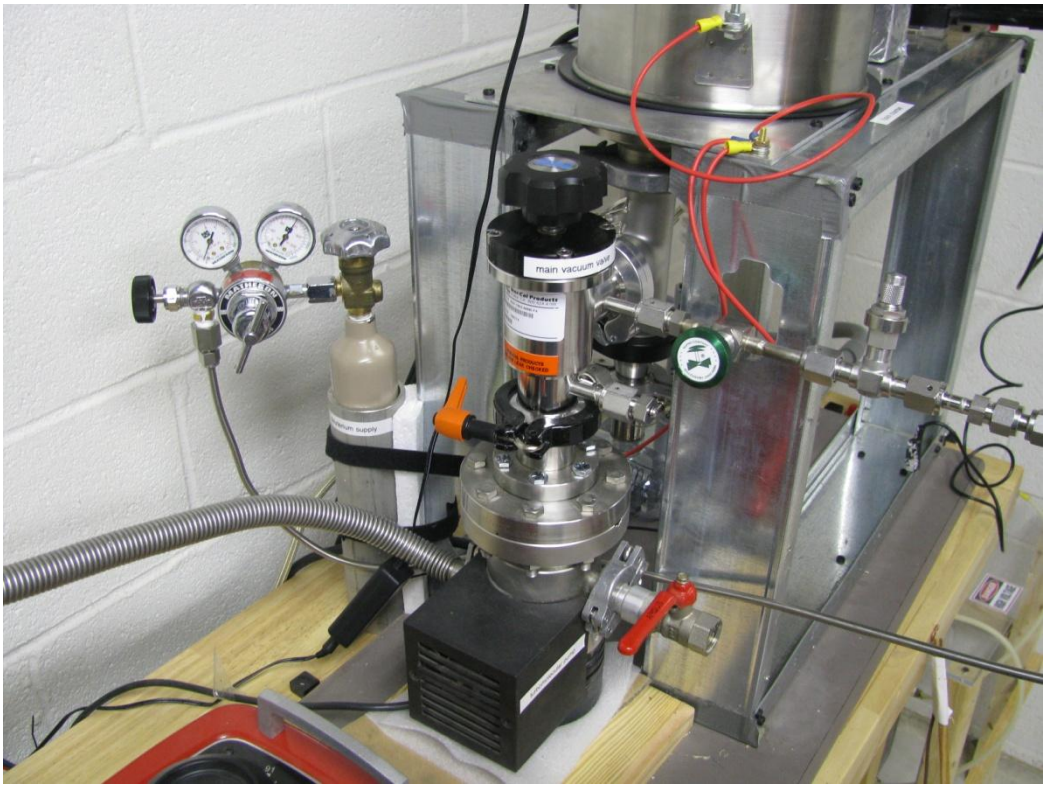

Figure 4 – Gas System. The deuterium bottle and regulator are at left in the picture. The stainless piping and needle valve are right of center.

b. Vacuum System and Fusion Chamber

Based on the Paschen discharge characteristics of deuterium, the IEC device pressure, depending on size, needs to be in the approximate range of 1 to 50 millitorr based on the Paschen curve and chamber size. Common mechanical, multivane vacuum pumps can achieve this pressure. However, if a vacuum chamber is not sufficiently conditioned by operation with much lower pressures, outgassing of contaminants like water molecules are expected (Hull, FAQ - Operation of a Fusor). Contaminant molecules could tend to collide with the

deuterium ions and prevent acceleration to fusion temperatures. In order to precondition, a pump capable of high vacuum operations was needed.

An Edwards RV3 mechanical roughing pump and Leybold Turbovac 50 turbomolecular pump were chosen because they were available from a previous science project and had been demonstrated to be capable of high vacuum conditions (see Figure 5).

In order to control the fusion chamber atmosphere a vacuum valve was needed to control flow of molecules out of the system. The fuel needle valve controlled the molecules going in. A bellows vacuum valve was obtained to control outlet flow (see Figure 5).

The IEC fusion chamber serves several purposes. The first purpose is to house the electrical grids. A glass bell jar was originally chosen because bell jars are inexpensive and easy to use. Because of safety considerations, the glass bell jar was replaced by a stainless steel vessel. Stainless steel does not shatter as a glass jar could. In addition, confined plasma can emit beams of electrons, which could rapidly heat a localized spot of a glass jar causing vessel failure (Donovan). Stainless steel can tolerate an ion beam without immediate failure. Another safety advantage of stainless steel is protection from x-rays. Energizing an IEC grid causes emission of x-rays of energy directly proportional to the applied

voltage. At voltages greater than 20 kV, the resulting x-rays can be hazardous. Stainless steel is an effective shield for x-rays in the range of planned voltage operation (Hull, FAQ - Operation of a Fusor).

Another advantage of a stainless steel chamber is that it can serve as the positively charged anode of the IEC device. A glass chamber would need a separate anode grid inside it (Ligon). For the device built for this project, a stainless steel pot was used. The size of a successful IEC chamber can vary from as small as less than 8 cm in diameter to much larger vessels as shown by the Paschen curve. If the chamber is used as the outer grid in the confinement, then the Paschen curve for the fuel must match the voltage range of the planned power supply and the vacuum to space relationship. For this project, a 21 cm diameter vessel was convenient and was expected to produce plasma over an achievable voltage range. The shape of the vessel was generally spherical with a cylindrical opening (see Figure 7). The vessel served as the anode for the system, and a ground strap was attached to set the DC system reference. Grounding the outer grid provided safety because the operator could easily come into contact with the chamber.

Examination of plasma for study was desired so a window was installed on the vessel. A 7.5 x 7.5 x 1.6 cm borosilicate glass window was installed on the vessel with a gasket to prevent in leakage. The thickness of the window was expected

to minimize chance of ion beam damage based on engineering judgment. A video camera was mounted above the window and connected to a remote monitor to allow plasma observation without direct exposure to x-rays.

The base plate of the vacuum chamber was aluminum which was chosen because it is easily machined. The base plate served as the point of most chamber penetrations including the pump off-take, instrumentation, and high voltage feed through.

The vacuum system parts were put together with KF type fittings, which clamp parts against a resilient centering ring preventing leaks. The chamber and window gaskets were made of Viton rubber, which is known to have low outgassing (Dupont). The gaskets were cropped to give minimal exposure in the chamber to prevent plasma break down of the hydrocarbons in the material. The gaskets were coated lightly with Apiezon vacuum grease for sealing. The vacuum grease was chosen for its low vapor pressure and therefore low outgassing.

Chamber pressure indication was needed in both the medium and high vacuum ranges. A thermocouple wide range vacuum gauge and controller was used for the medium range. The medium gauge range was used for most of the reactor operations which occurred in the millitorr range. For the higher, conditioning,

range, a glass ion gauge and controller with a range of 10^{-12} to 10^{-5} torr was used (see Figure 6).

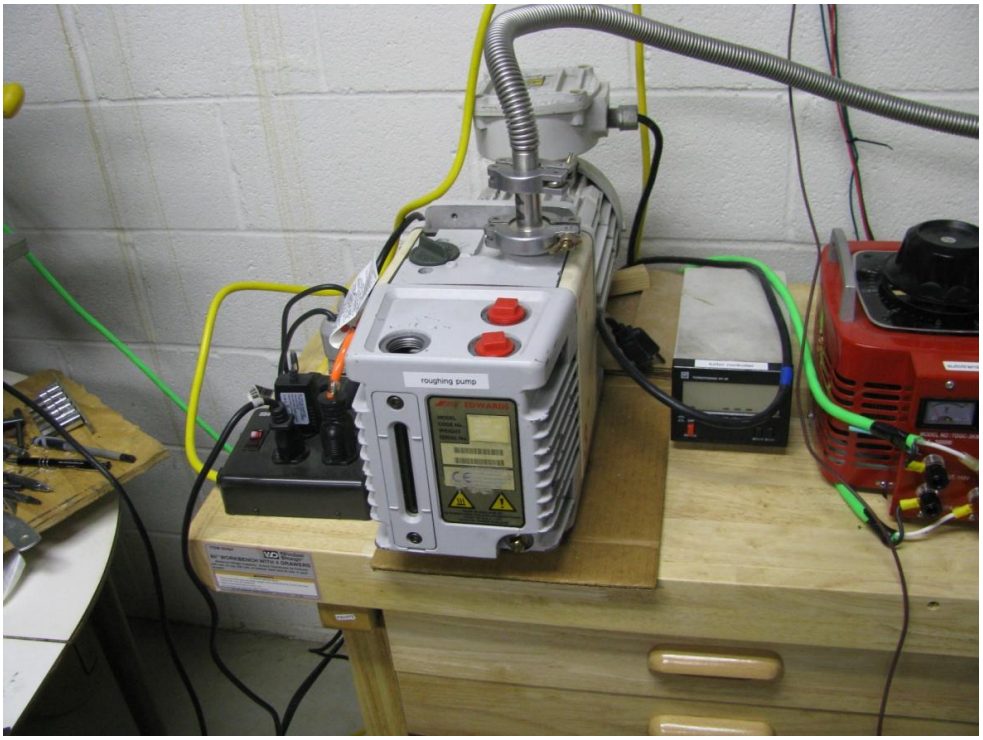

Figure 5: Mechanical vacuum pump.

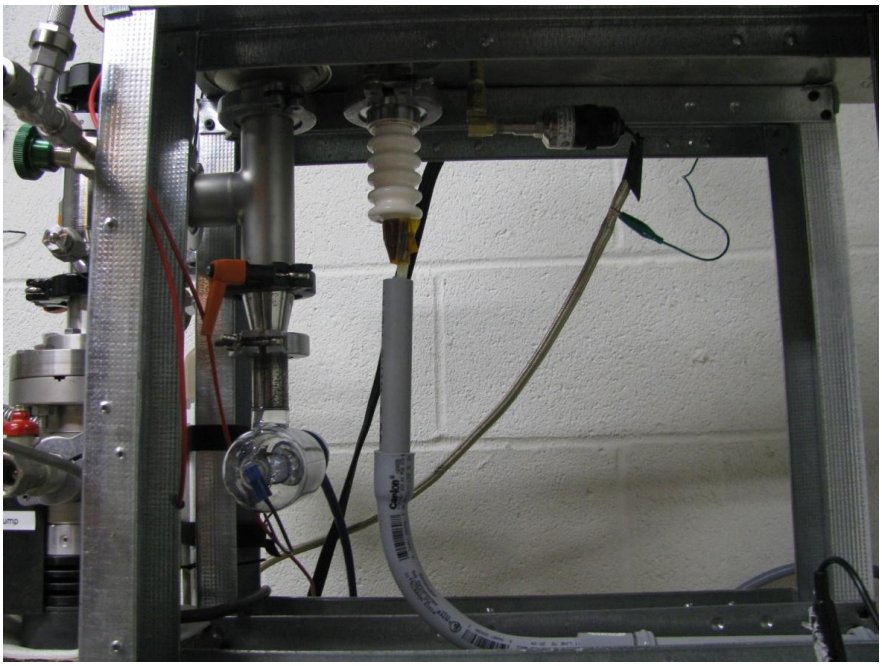

Figure 6: Base of Vacuum System showing turbo pump and valves at left. The glass ion gauge is near center, and the thermocouple pressure gauge is the horizontal probe at the top of the picture.

Figure 7 – Fusion Chamber, glass window, turbo pump, and vacuum valve

c. High Voltage System

D – D fusion can occur in an IEC device at voltages as little as 10 kV or less, but detectable fusion generally does not occur until voltages are at least 15 kV (Hull, FAQ - Operation of a Fusor). Preassembled power supplies are available but expensive. For this project, a negative DC power supply was built. The power supply needed to take household power at 120 VAC and convert it negative DC at a variable voltage up to 30 kV with a positive ground. Current would be up to 20 mAmp. The transformer from an x-ray machine was purchased as the primary component (see Figure 9). To vary voltage to the x-ray transformer, a 0 to 120 VAC adjustable autotransformer was used (see Figure 11). High voltage diodes converted the transformer output to negative DC. A high voltage capacitor filtered ripple remaining in the rectified output of the diodes. A high resistance power resistor was used as a ballast to prevent surges from damaging the transformer. The transformer and diodes were immersed in transformer oil to reduce potential for arcing.

Understanding voltage and current was essential to reactor operation to monitor plasma status and grid health to prevent overheating. A high resistance voltage divider and panel meters were used, and a regulated 5 VDC power supply powered the instrument displays. The voltage divider allowed use of a low voltage meter by tapping the divider string at a 10,000 part fraction of the total voltage drop.

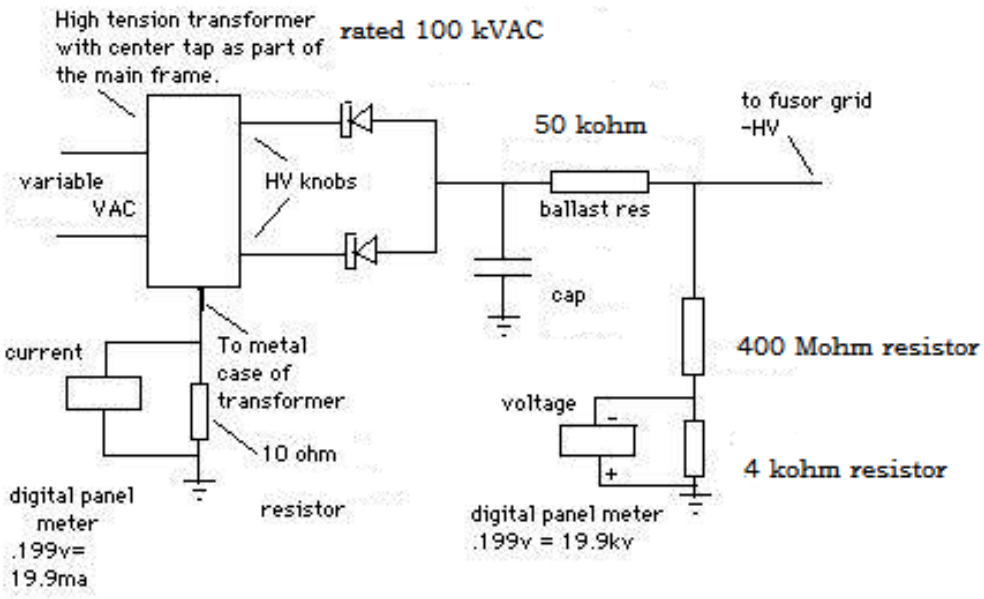

Figure 8 – power supply schematic

The power supply was connected to the fusion chamber and inner grid using high voltage cabling. Exposed electrical connections were coated with dielectric grease or polymide tape to prevent corona and arcing.

A high voltage rated vacuum feed-through was used to port the power into the inner grid. Inside the chamber, an alumina insulated stem positioned the inner grid at the center point of the chamber.

The grid was made of .0114 cm thick tungsten wire shaped into circles chosen to be one fifth of the chamber in size (see Figure 10). The chamber diameter was 21 cm so the grid diameter was 4.2 cm. The inner grid needed to be both

symmetrical and transparent. Current IEC research shows that fusion efficiency is enhanced by transparency of at least 92 percent (Donovan). The inner grid is 99.18 percent transparent with three loops as calculated by comparing the cross section of the total grid wire used to the surface area of the grid sphere.

Grid Area = diameter x π x number of wire loops

4.2 cm x π x 3 x 0.0114 cm = cross section of wire = 0.45 cm^2

Grid Surface Area = 4 x π x $radius^2$

4 x (4.2 cm / 2)^2 x π = surface area of grid sphere = 55 cm^2

(55 cm – 0.45 cm) / 55 cm = .99 transparency

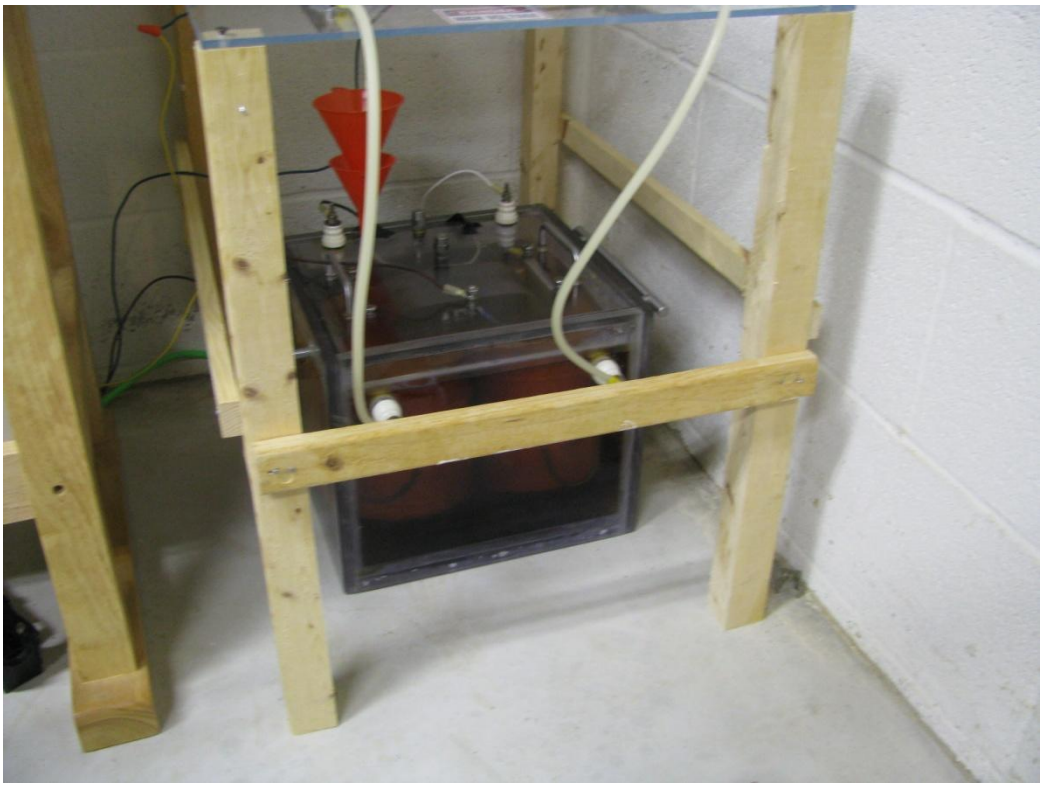

Figure 9 – high voltage transformer

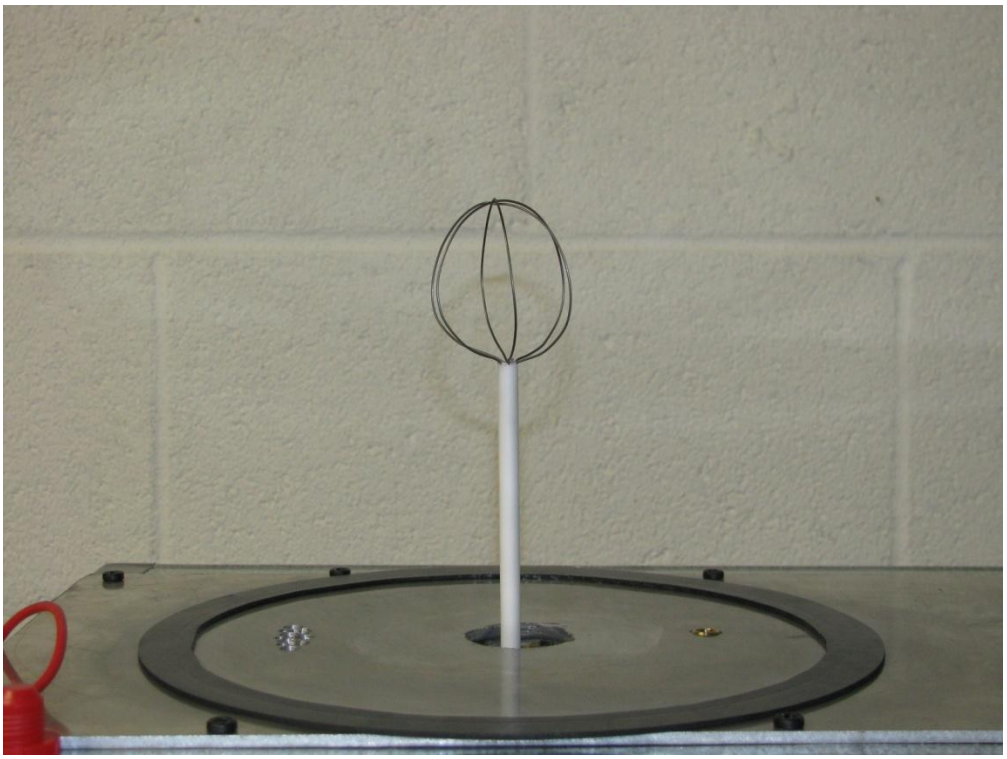

Figure 10 – Inner tungsten wire grid on alumina stem with fusion chamber removed.

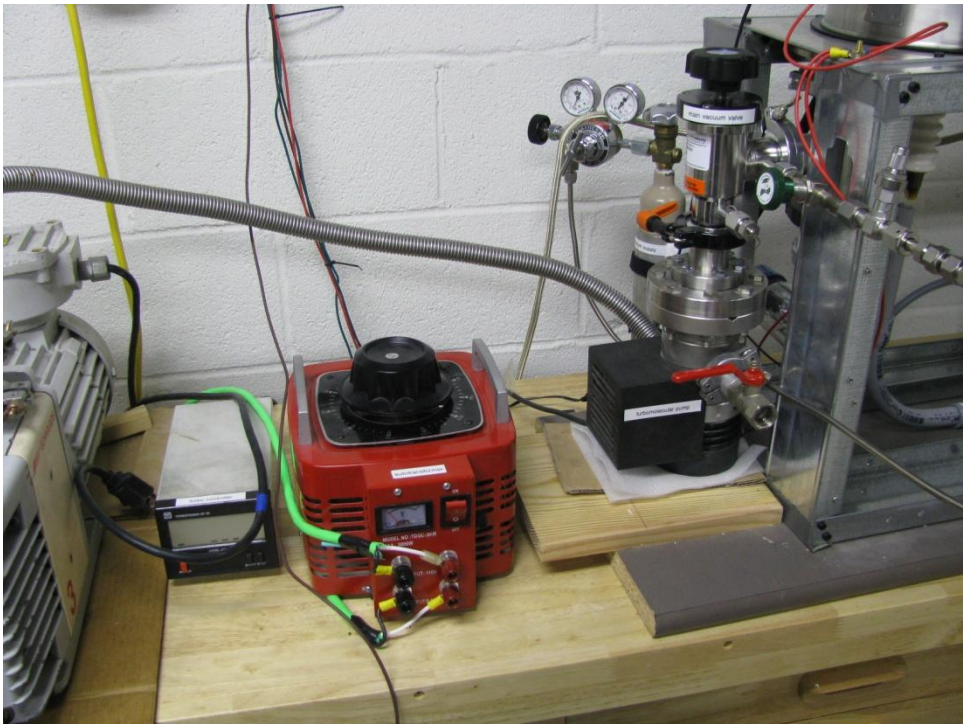

Figure 11 – 120 Volt Autotransformer used for voltage control

d. Neutron and Radiation Detection

Deuterium fusion will produce neutrons and detecting resultant neutrons provides the most credible proof that fusion has occurred because natural sources of neutrons are not significant. Detecting neutrons is not easy because neutrons have no charge, and detecting secondary evidence of neutrons after they interact with other materials is easier (Knoll). An Eberline PNC 1 (see figure 12) Portable Neutron Counter was obtained. The PNC 1 counter uses a BF_3 (Boron trifluoride) gas filled proportional ion chamber. The ion chamber is mounted in a paraffin block which slows neutrons down to optimal levels for reaction with the boron in the fill gas. When a boron 10 atom absorbs a neutron, energy is released which causes an electrical pulse counted by the detector.

Figure 12 – PNC 1 Detector at right

An alternate approach to neutron detectors is activation analysis. This method relies on allowing the high energy neutrons released by fusion to slow down in a thermalizing material. The thermalized neutrons would then be absorbed by a target material with a high absorption cross section. The target material would then be mildly radioactive and could be measured with radiation detection. For this project, a thermalizer was made using high density polyethylene (HDPE) plastic which readily slows neutrons. A piece of silver was used as a target because it easily absorbs neutrons, and its subsequent radioactive decay can be measured. An activation chamber was made HDPE with another layer behind the silver target to serve as a reflector (see figure 14). Figure 13 shows that a peak capture rate is obtained with a 3.89 cm layer of HDPE. This detection method involves positioning the HDPE as close to the neutron source as possible for several minutes and then quickly measuring the silver for radioactivity.

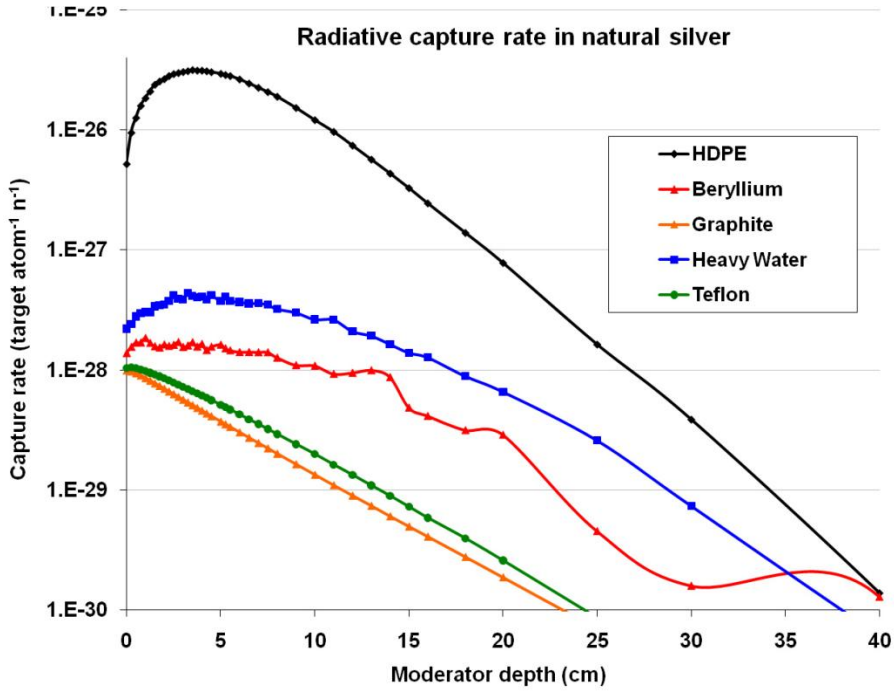

Figure 13 – Cross section plots of various thermalizing media (Willis)

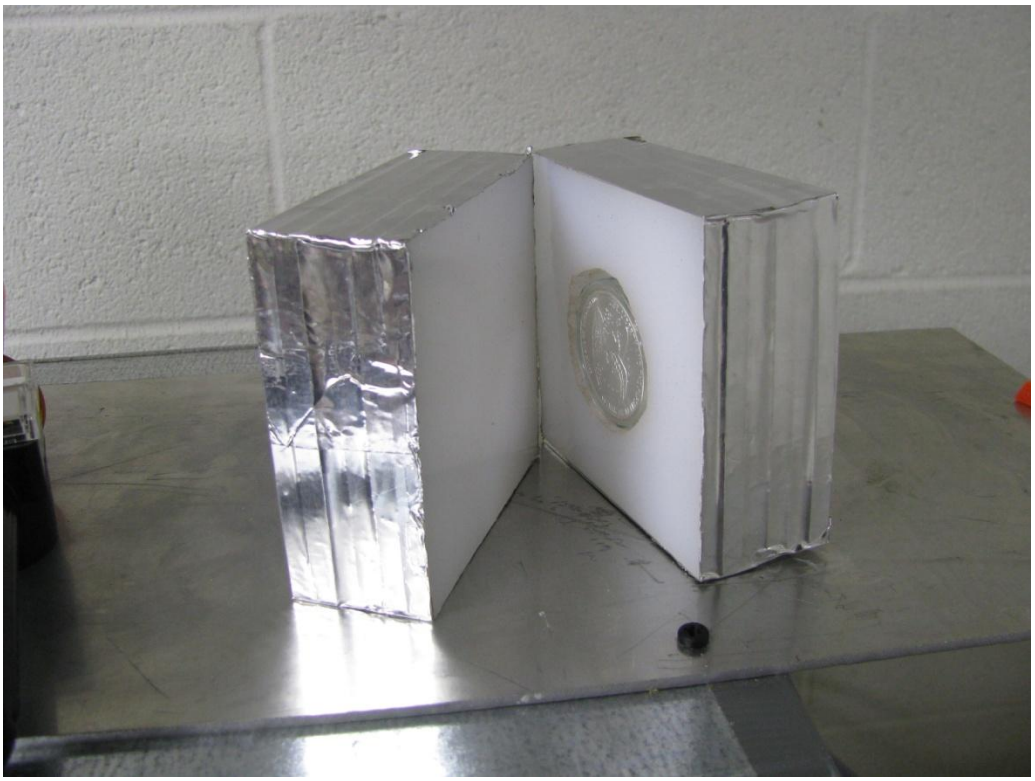

Figure 14 – Thermal activation chamber open to show sandwich of HDPE and silver

Radiation detection was used as a safety precaution so x-ray levels were known at higher voltage operation. For this project, a goal of zero exposure for personnel was set. A pencil dosimeter and a sensitive Geiger Muller radiation detector were used to verify low dose rates.

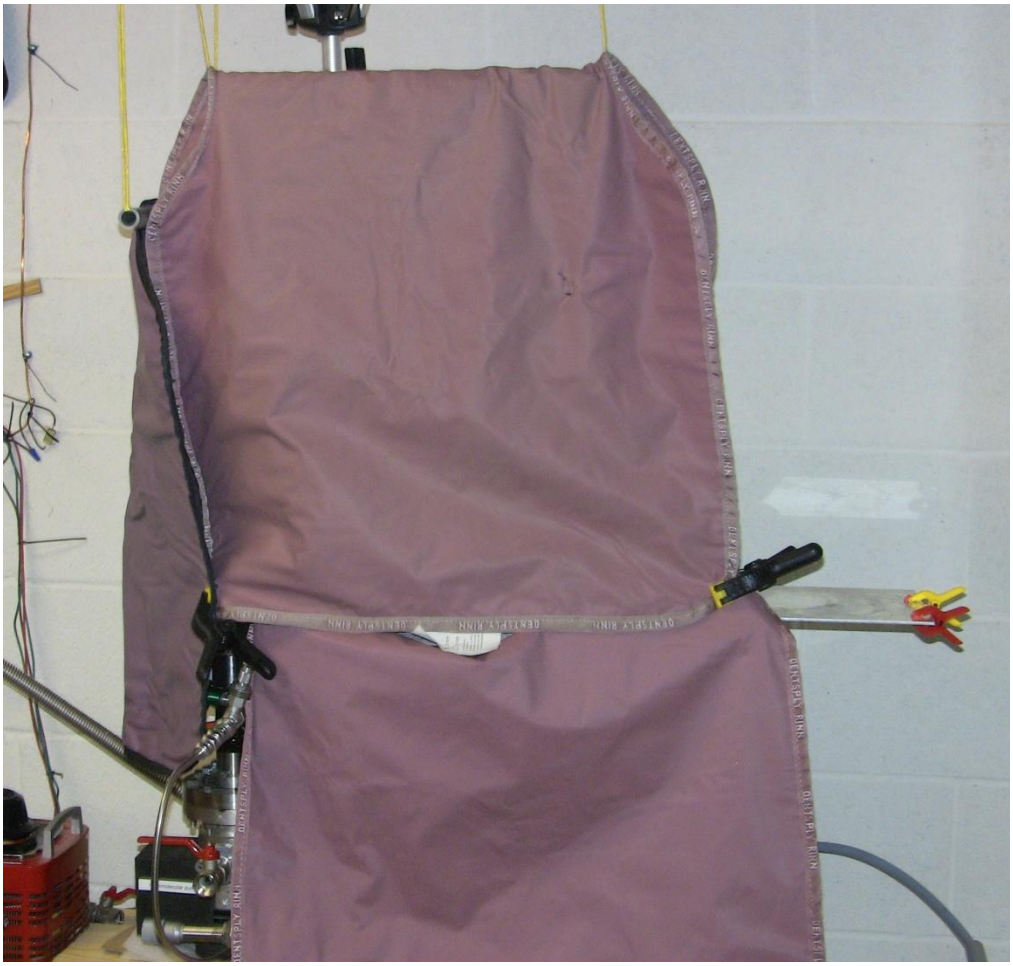

Figure 15 – Radiation shields installed around the chamber reduced operating area radiation to normal background levels.

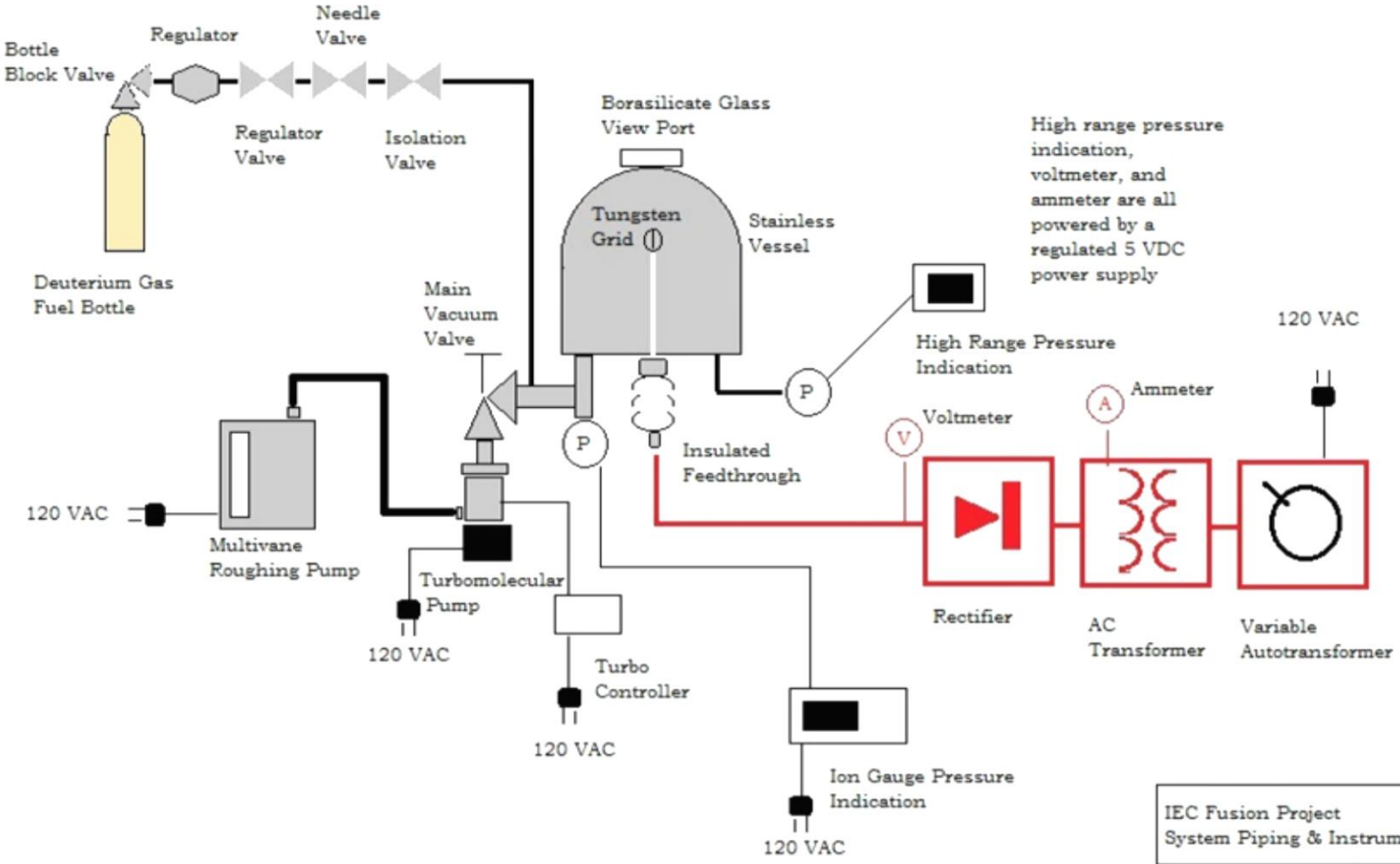
Bottle
Block Valve
Regulator
Needle
Valve
Regulator
Valve
Isolation
Valve
Deuterium Gas
Fuel Bottle
Borasilicate Glass
View Port
Tungsten
Grid
Stainless
Vessel
High range pressure
indication,
voltmeter, and
ammeter are all
powered by a
regulated 5 VDC
power supply
Main
Vacuum
Valve
High Range Pressure
Indication
P
120 VAC
Ammeter
A
Voltmeter
V
Insulated
Feedthrough
120 VAC
Multivane
Roughing Pump
Turbomolecular
Pump
120 VAC
Turbo
Controller
120 VAC
Rectifier
AC
Transformer
Variable
Autotransformer
Ion Gauge Pressure
Indication
120 VAC
IEC Fusion Project
System Piping & Instrumentation
Schematic only;
Not to scale
12/2011

C. Methods

a. Apparatus Component Procedures

Correct use of the various components of the fusion reactor system is critical for both safety and function. Because actions must be completed in a careful sequence, systematic checklists were developed and used throughout this project. The following summarizes the component procedures:

Safety – Before the start of each evolution, a safety inspection was performed. In all cases, the adult mentor oversight was required. The room and equipment was cleared of unnecessary materials and personnel. A fire extinguisher rated for class A, B, and C fires was obtained and verified charged prior to each evolution. When voltage operation greater than 15 kV was planned, a Geiger counter was inspected and battery tested. A self-reading dosimeter was read and zeroed as needed. Blankets equivalent to 3 mm of lead were hung around the chamber (see Figure 15). During operation at higher voltages, frequent surveys for radiation were made. It was expected that the student experimenter would receive no radiation exposure. A camera was mounted over the chamber viewport. A monitor connected to the camera prevented direct exposure to soft x-rays expected at the viewport during operations above 20 kV. Finally, a pre-job brief was conducted with the adult mentor to receive concurrence on experimental goals, potential hazards, and contingency actions. The primary

contingency action was opening of the autotransformer electrical source. A one-hand operation only rule was used to minimize consequences of accidental contact with high voltage conductors.

Vacuum System – The vacuum system was used to remove contaminant molecules from the fusion chamber and to control the deuterium pressure. The oil level in the roughing pump was checked prior to each run. Pressure indication was energized first and verified operable. Next, the roughing pump was started and slowly aligned to the chamber by opening the main vacuum valve. The gas injection line was aligned to the vacuum system during the roughing period to remove residual gases if the previous run was done with a different gas than the planned one. Chamber pressure was roughed to below 25 millitorr in preparation for turbomolecular pump operation. The turbo pump cannot tolerate operation above 50 millitorr because of possible blade damage. Once the roughing pressure was achieved, the turbo pump cooling fan was started followed by start of the turbo pump itself. When the turbo pump reached normal speed of 7200 rpm, chamber pressure was expected to be well below the low range of the thermocouple vacuum gauge. At this point, the ionization gauge would be turned on. The ion gauge was turned off any time pressure was raised above 1 x 10-4 torr. Prior to chamber plasma operations, pressure was typically reduced to below 3 x 10-6 torr.

Electrical System – Prior to energizing the grid electrical system, the high voltage transformer, rectifier, and autotransformer were all physically inspected to verify no foreign material and proper routing of cables. The autotransformer dial was verified at the zero position. An independent, 20 amp, 120 VAC circuit was used for the autotransformer to ensure that any surges that tripped the circuit breaker would not interrupt power to the remainder of the fusion system components. The autotransformer on-off switch was the primary switch for the system, and was the major emergency stop method for the fusion device. The dial on the autotransformer was raised and lowered as needed. Digital indicators for voltage in kilovolts and current in milliamps were used. Upper limits for voltage were set for each experiment and in all cases, 20 milliamps was the steady state current limit.

Gas System – The gas injection system was normally aligned to the deuterium bottle and regulator. Preliminary experiments were performed using air and helium, and in these cases, the injection line was disconnected before the needle valve to allow injection of the alternate gases at this point. During deuterium operation, the regulator outlet valve started as closed. The gas outlet valve was briefly opened and reclosed to pressurize the regulator. The small amount of gas between the bottle and regulator outlet valve was expected to be sufficient for all fusion runs, and closing the bottle valve prevented inadvertent wasting of deuterium fuel through misalignment or valve failure. The gas regulator was set

to approximately 2 psig. Large differential pressures across the needle valve would give injection control that was too coarse. During plasma and fusion operations, the needle valve was the normal control of gas insertion.

b. Comprehensive Experiment Procedures

The initial experimentation was designed to demonstrate that the chamber and grid produced controllable plasma. Therefore, the procedure would resemble normal fusion operation, but focused on non-fusion fuels and lower voltages.

Experiment 1 – Air Plasma

Chamber pressure was reduced to eliminate contaminants. The system voltage was set at -5 kV with no plasma expected. Next, the main vacuum valve was throttled to limit molecule removal. A small amount of air was admitted using the needle valve until pressure started to rise. The camera monitor and current indication was watched for expected plasma indications. When plasma was seen visually and through rising grid current, pressure was stabilized with the needle valve and with the main vacuum valve. Observations were recorded for plasma characteristics including color and shape. Stable combinations of current, pressure, and voltage were recorded. Voltage, current, and pressure were varied to determine effects on the plasma.

Experiment 2 – Helium Plasma

The helium plasma experiment was the same as the air plasma experiment except that helium gas was injected instead of air.

Once chamber operation experience was gained through repeating experiments 1 and 2, deuterium experiments were designed and conducted. Similar to the air and helium runs, information about deuterium plasma was desired especially when it could provide evidence that the chamber could be successful in achieving conditions for fusion. After data was obtained by the initial deuterium runs, subsequent runs were designed to achieve and measure fusion.

Experiment 3 – Deuterium Plasma

The deuterium plasma experiment was the same as the air plasma experiment except that deuterium gas was used and the original starting voltage was -10 kV. Experiment 3 was repeated several times. This was needed to condition the chamber. Small amounts of contaminant material like vacuum grease, fingerprints, gasket material, and water molecules on chamber surfaces caused small electrical discharges that momentarily disturbed the plasma. These small discharges gradually stopped as the plasma conditioned the surfaces.

Experiment 4 – Paschen Discharge Measurement

The voltage required to initiate plasma varies with vacuum, distance, and the gas. This experiment was designed to determine if the chamber design produced a relationship that resembled known characteristics for deuterium. This was important because the ability to produce fusion relies on the ability to control the plasma. In this experiment, the needle valve was set at a small deuterium injection rate, and the pressure was varied using the main vacuum valve. At incremental pressures, the voltage was slowly raised using the autotransformer until current and plasma was observed. The voltage was recorded at each pressure increment until voltage was -20 kV. Experiment 4 was also conducted using air as a control.

Experiment 5 – Deuterium Emission Spectrum Measurement

The color of a plasma is characteristic of the excited electron emissions for an element (Martin). By examining the chamber's plasma light spectrum during deuterium operation, the predominance of deuterium emission versus plasma created by contaminants can be confirmed. Experiment 5 used a digital spectroscope to collect light intensity at different wavelengths. The plasma was established using Experiment 3 methods at -12 kV and star mode operation. Star mode refers to symmetrical plasma that is tightly confined inside the inner grid (Plasma-Universe). A SpectroVis Plus spectrometer was used for the measurements.

Experiment 6 – Silver Activation

The aim of this experiment was to use byproduct neutrons for material activation. The neutrons from deuterium fusion have an energy level of 2.5 MeV. Higher energy neutrons like this are difficult to detect until they reach energies near thermal equilibrium with surroundings. At thermal energies, neutrons are more readily absorbed by some elements (Knoll). When a neutron is absorbed, the nucleus is said to be activated because in nearly all cases the resulting material is radioactive (Knoll). Detecting the presence of activated materials is easier than detecting the neutrons themselves. Elements with high cross sections for neutron absorption that also produce radioactive elements with half-lives that are convenient are best. Naturally occurring silver is ideal for this experiment for those reasons. For a given neutron flux, approximately ten minutes of exposure will produce a peak activity in the silver with resulting radioactive isotopes that decay slow enough to detect (Hull, FAQ - Activation Materials - Silver). Naturally occurring silver has two main isotopes, Ag 107 and Ag 109. Both isotopes have relatively high cross sections for thermal neutron absorption, and produce resulting isotopes of Ag 108 and Ag 110 respectively. Ag 110 decays very quickly with a 24 second half-life, but Ag 108 has a 2.5

minute half-life with detectable beta particles (Hull, FAQ - Activation Materials - Silver).

A coin of pure silver was sandwiched between two slabs of high density polyethylene and positioned at the surface of the fusion chamber. The stainless steel wall of the chamber is permeable to fast neutrons. Then, deuterium plasma was established in the chamber. Various voltages were attempted, but measurable fusion was not expected until voltage was at least -20 kV. After 10 minutes of operation, the fusion chamber was shutdown and the coin was quickly placed on a Geiger counter and monitored.

Experiment 7 – Deuterium Fusion Neutron Counting

This experiment was designed to provide ultimate proof of nuclear fusion by observing the presence of fusion byproducts. Of the fusion byproducts, only neutrons would be expected to pass through the fusion chamber walls. Protons, Helium 3, and tritium would react with the atoms in the stainless chamber. Neutrons because of their energy and neutral charge would pass through. There are very few sources of neutrons in background radiation. Therefore, the presence of neutrons significantly over background levels would be positive indication of nuclear fusion. This experiment varied voltage, current, and deuterium pressure to determine effects on neutron levels using the PNC 1 counter.

D. Results and Data

a. Analysis of Data

Experiment 1 – Observations

- Plasma first ignited with a blue glow that was faintly visible inside the inner grid (see Figure 17).
- Raising voltage intensified the light of the plasma and changed the shape. With rising voltage the plasma was round with a bugle shaped light on one side. Further increases in voltage caused the plasma to shrink but intensify in brightness in the center. The bugle shaped portion of the ball narrowed to a thin line emanating outward to the chamber wall. The color of the plasma changed to a more purple color (see Figure 18). The chamber became hot to the touch especially at the point where the beam met it. These observations compare with plasma characteristics known as glow mode, bugle mode, and jet or ion beam mode (Plasma-Universe).
- Stable combinations of parameters included -3 kV, 17 millitorr, and 17 mA. Other combinations could be controlled. Another recorded combination was -1.91 kV, 6.3 mA, and 18 millitorr.

- A small amount of helium was sprayed in the air immediately adjacent to the gas inlet, and the plasma immediately extinguished. This was expected since helium has a higher ionization voltage at lower pressures than does air (UK). This also confirmed that the chamber was causing ionizations on the left side of the Paschen discharge curve.

Figure 17 – Air plasma in 'glow mode.'

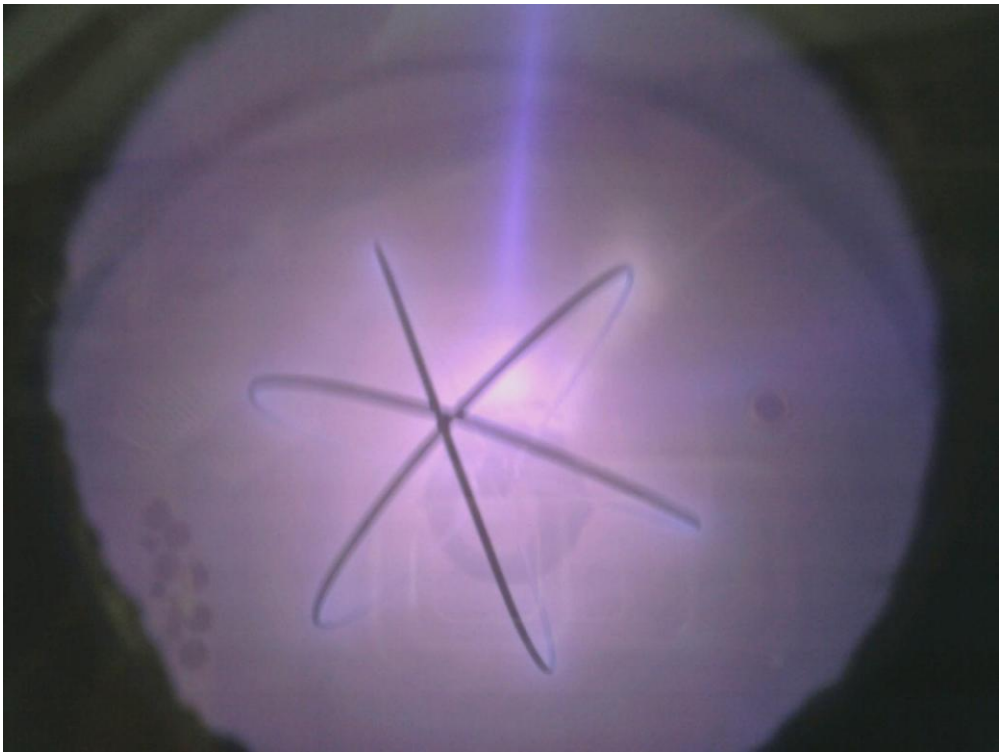

Figure 18 – Air plasma in ‘jet mode’ also known as ion beam mode.

Experiment 2 – Observations

- Plasma ignition and observations for helium were very similar to observations made for air. The color of the plasma was a pink-purple with thin blue edges near the chamber walls and ion beam (see figure 19).
- Stable combinations of parameters included:

-5.44 kV	8.60 mA	15 militorr
-7.02 kV	5.17 mA	8 millitorr
-6.16 kV	8.64 mA	8 millitorr
-4.92 kV	12.27 mA	6 millitorr
-4.05 kV	16.60 mA	10 millitorr

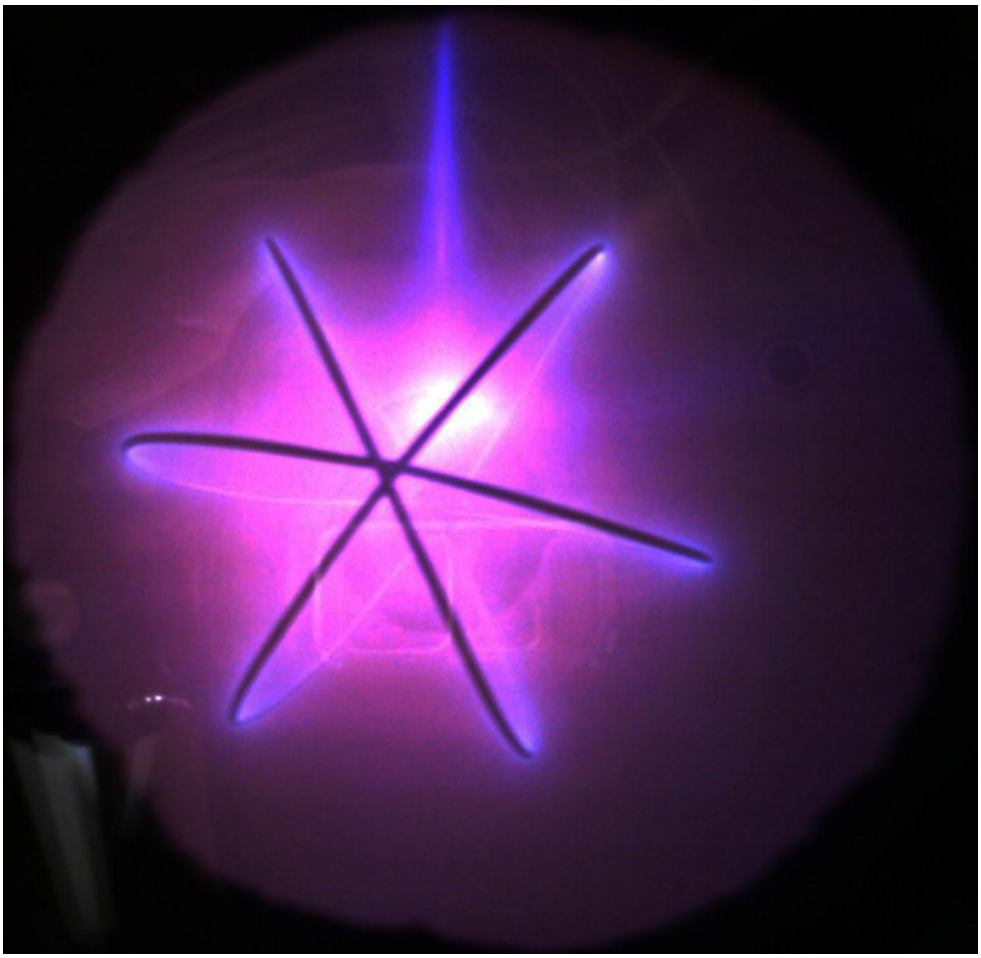

Figure 19 – Helium plasma showing color intensity near the center of the grid and an ion beam.

Experiment 3 – Observations

- Plasma ignition and observations for deuterium were very similar to observations for air and helium. The color of the plasma was pink. It was also observed that digital cameras saw the color as deep blue, but the naked eye saw the color as pink. It is likely that this difference is related to emission of infrared light not seen by the eye but recorded by a digital camera as blue. This was confirmed by testing the camera with an IR

remote control which gave a blue light in images. Later experiments made use of cameras that were more true in color. Stable combinations were not recorded because higher voltages produced arcing and instrumentation noise. The stability data was used to make improvements to the high voltage system and to add shielding to the instrumentation.

- Multiple repetition of Experiment 3 yielded more stable conditions and higher obtainable voltages. In addition, a plasma configuration known as star mode was routinely observed. In this mode, symmetrical ion beams were seen at each open point in the inner grid (see figure 20).
- A light coating of tungsten became deposited over time inside the chamber (see figure 21). This was from high temperature sputtering of the tungsten grid.

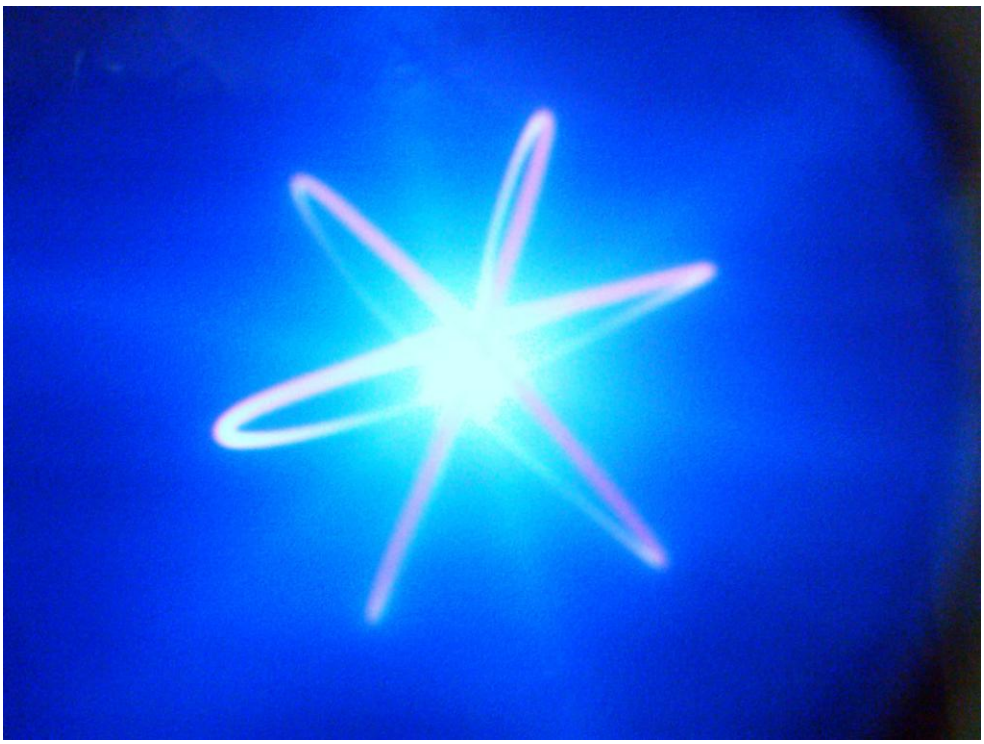

Figure 20 – Deuterium plasma in ‘star mode’ indicated by intensely confined plasma at the center of the grid with spoked ion beams.

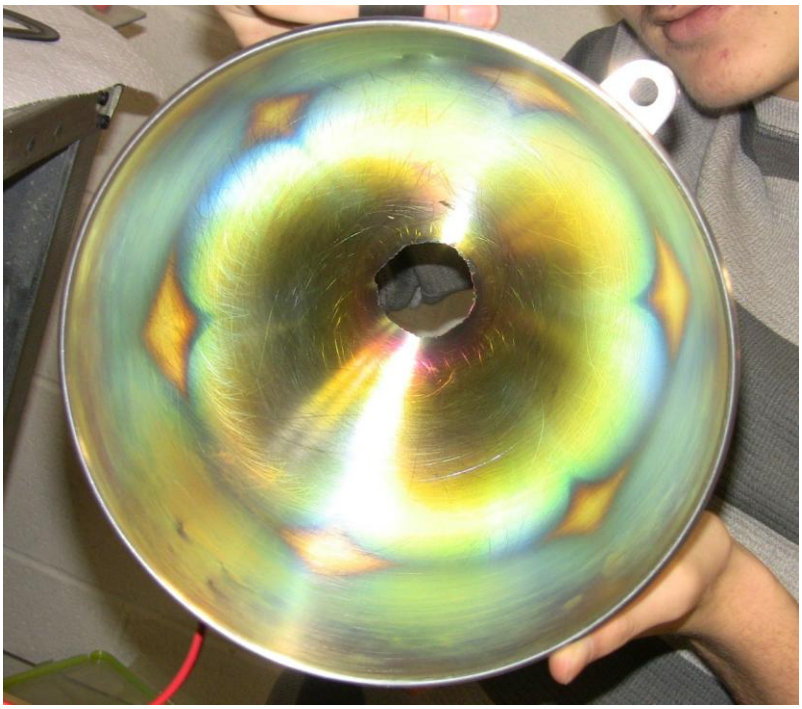

Figure 21 – Tungsten deposition on inside of fusion chamber. The deposition shape shows influence of the grid design.

Experiment 4 – Observations

- The following data was collected for plasma initiation:

Air

Pressure in millitorr	Voltage at first glow in –kV DC
6	1
4	2
2	2.5
1	3
0.3	5
0.2	>20

Deuterium

Pressure in millitorr	Voltage at first glow in –kV DC
46	4
44	4.5
42	5
40	5.5
38	6
36	6.5

34	7
32	8
30	9
28	10
26	12
24	13
22	15
18	18
16	20
14	>20

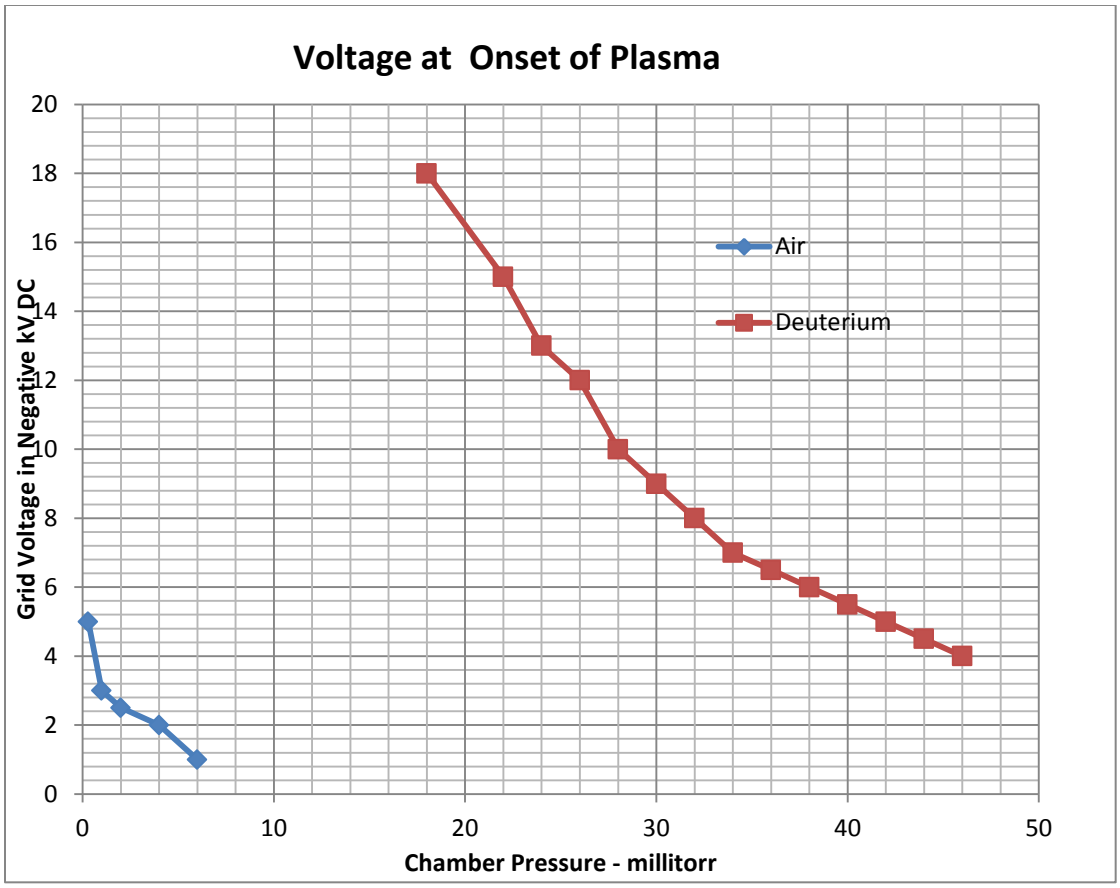

Figure 22 - Recorded plasma onset voltages

- The discharge voltage plots for air and deuterium strongly resemble the known Paschen discharge behavior for these gases. This confirmed the performance region of the device and because IEC fusion was originally conceived to occur in this region, the data supports use of the chamber for fusion.

Experiment 5 – Observations

Recorded emission peaks showed that hydrogen was in the plasma. It is likely that deuterium isotope was the source of the hydrogen spectrum because there is no known source of normal hydrogen contamination.

Figure 23 is the spectrum recorded for this experiment, and the largest spike is at 656.4 nm. This corresponds to the D_α emission spike known for deuterium (see Figure 24) (J. E. Martin).

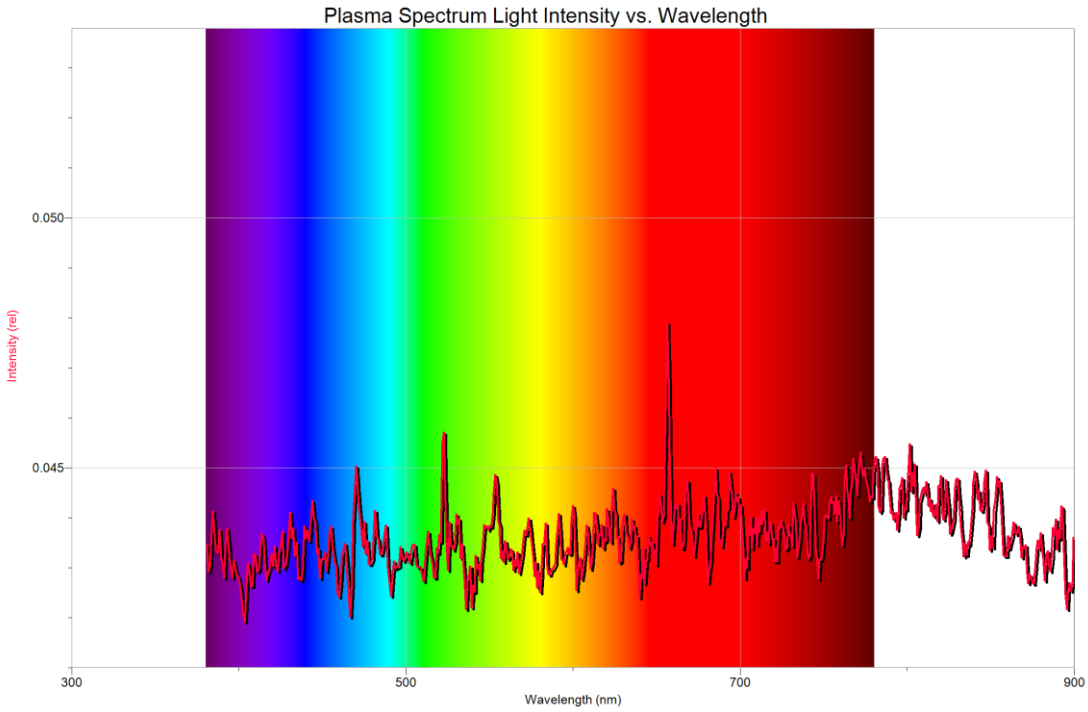

Figure 23 – Recorded Plasma Spectrum

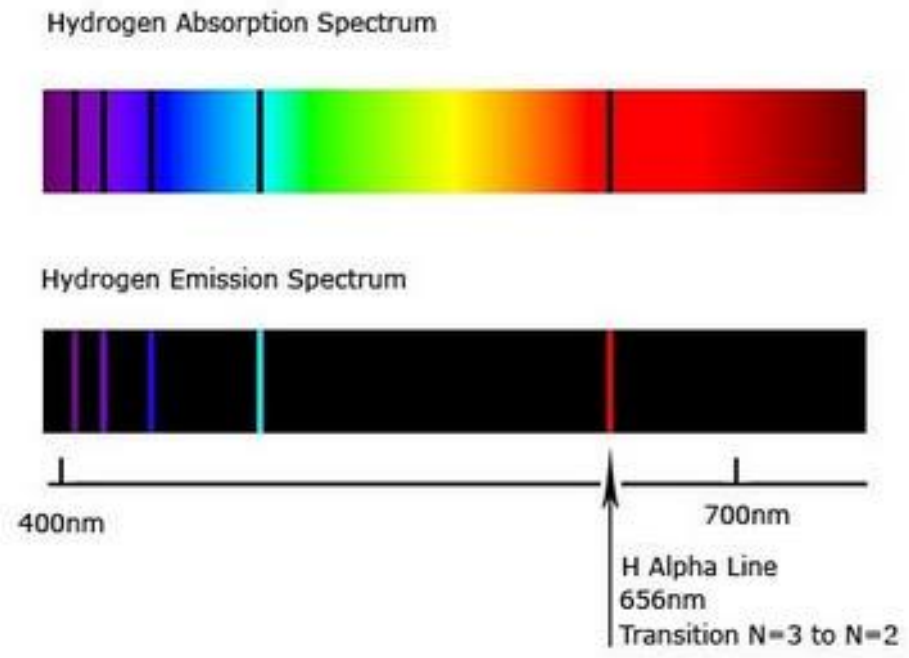

Figure 24 – Known emission lines of hydrogen for comparison (South-Oakleigh)

Experiment 6 – Observations

More than a dozen separate reactor plasma operations spanning several hours of total operation were performed. During these runs, observations of pressure, current, and voltage control stability were made. The upper voltage limit of the chamber was sometimes found through observations of internal arcing that disrupted the plasma. With operation time, the upper voltage limit would rise as the chamber apparently conditioned. Steady state operation at -25 kV was not attained for experiment 6. The highest steady state voltage was -23 kV. When the silver was surveyed after a run, no counts above background were seen. Radiation surveys of the chamber showed the presence of x-ray radiation at voltages exceeding 18 kV. This was expected given the similarity between x-ray

tube construction and the construction of this fusion reactor. Surveys also showed that the shielding hung around the apparatus were effective in eliminating exposure for the experimenter during fusion operations.

Experiment 7 – Observations

Experiment 7 was conducted after modifications were made to the inner grid that improved the connection between the grid and the supply stalk. This significantly reduced arcing and therefore raised the attainable voltage. Neutron background levels were not significantly above zero counts per minute (cpm) on the PNC-1. At -25 kV, 8 mA, and 16 mtorr, neutron levels were 60 cpm. This measurement confirmed that nuclear fusion was achieved. Once this measurement was taken, the following data was taken for various conditions:

Voltage –kV dc	Current milliamps	Pressure millitorr	Neutrons cpm
16	11	18	10
17	10	18	12.5
18	7	17	15
18	11.2	18	20
19	9.5	16	20
19	11.5	16	25
21	10.8	16	40
23	8.1	15	40
22	13.1	15	50
25	8.1	14	60
25	11.9	14	100
26	9.4	13	100
27	5.4	13	100
28	8.4	13	120
29	9.6	13	120
31	10.8	13	130

Figure 25 – Neutron readings versus other chamber parameters.

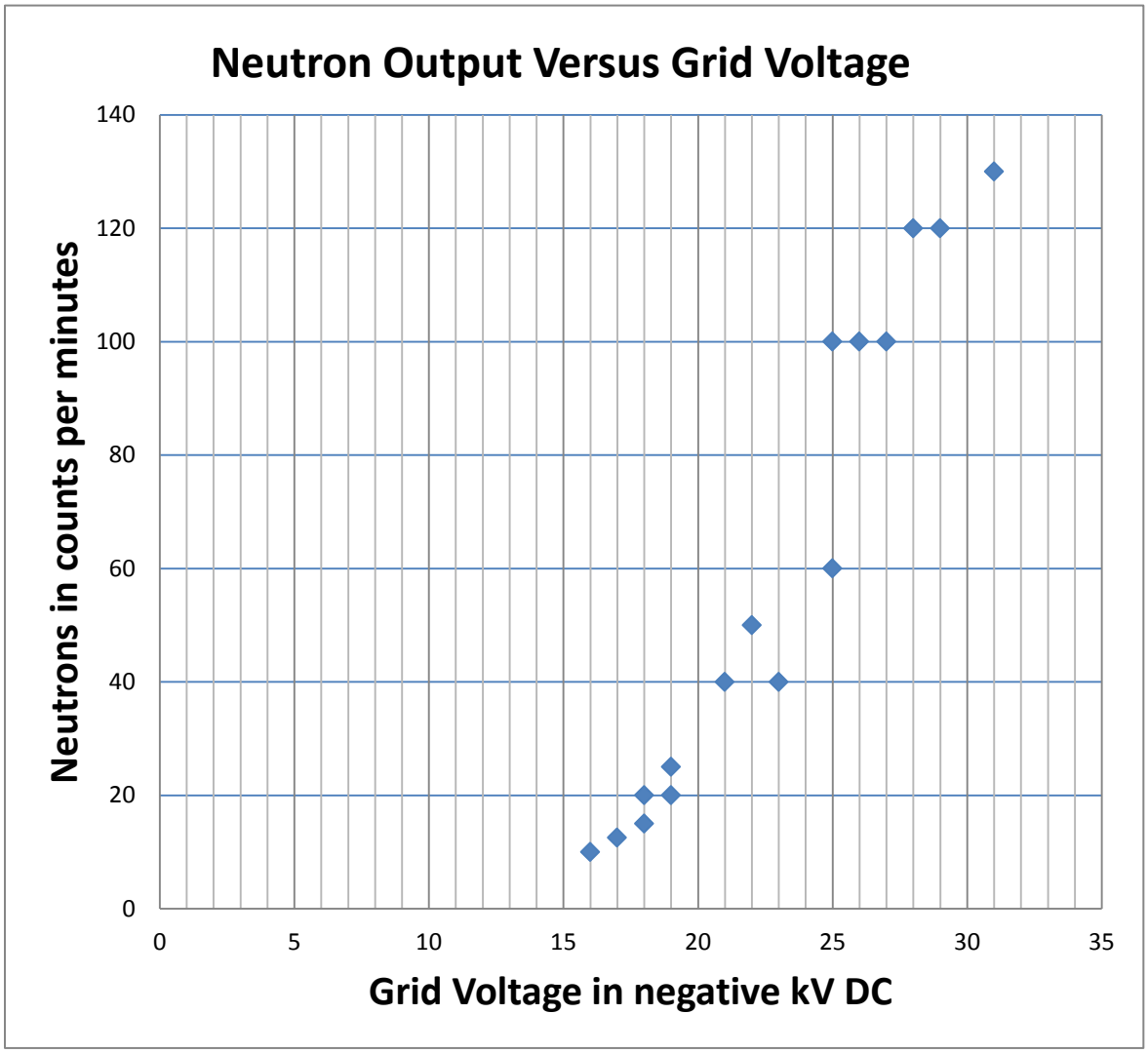

Figure 26 – Neutron counts versus grid voltage

The most significant influence on neutron count rate was voltage, but for a given voltage, higher currents which are indicative of greater fuel density, also raised neutron levels. This was expected because the likelihood of fusion is known to go up with voltage and fuel density.

Control tests to confirm the presence of neutrons were performed. The first of the confirmatory tests was through the use of air as a fuel instead of deuteriurm.

Air was induced to plasma with -25 kV dc, and neutron indication was zero. The other confirmatory test was done during a deuterium run. With 60 counts per minute indicating on the PNC-1, the BF3 tube was removed from the paraffin block moderator. The count rate dropped to zero. When the tube was returned to the moderator block, counts returned to 60 counts per minute. This confirmed normal response of the neutron indication. This test also indicated that the neutrons coming from the chamber were of fast or high energy. The expected energy of fusion neutrons is 2.5 MeV and a BF3 detector cannot sense neutrons until they have been slowed by a moderator (Knoll).

Multiple fusion runs were conducted. The highest neutron count rate observed was 150 counts per minute at -30 kV (See figure 27).

Figure 27 – Maximum neutron count rate recorded

Based on a calibration sheet provided with the PNC-1 detector, 150 counts correspond to a dose rate of 1.6 mRem/hr. The conversion for dose rate to neutron flux for 2.5 MeV neutrons is 29 $X10^6$ neutrons/cm2 for each Rem. (USNRC).

The flux at the detector is therefore-

1.6 mRem/hr x 29 $x10^3$ neutrons/cm2 x 1 hr/3600 sec = 13 n/cm2 –sec

Assuming a spherical and uniform neutron emission from the center of the grid, the total neutron production rate can be calculated. The detector tube was located 16 cm from the center of the grid. Using this as the radius and the surface area of a sphere as $4\pi r^2$, the total neutron generation rate per second is

13n/cm2 – sec x 4 x π x 16 cm x 16 cm = 42,000 neutrons/sec

Because neutrons come from 50 percent of all deuterium fusions, the fusion rate is 82,000 fusion events per second.

During one of the fusion runs, an unexpected observation was made. During operation at -30 kV, the inner grid was observed to spontaneously spin clockwise 60 degrees before stopping. All possible explanations would have to assume that the grid came connection came loose from thermal expansion, but the reason the grid moved and stopped is uncertain. One possible explanation would be that coulombic forces moved the grid into a static equilibrium. This is the first documented observation of electromechanical motion in a fusion reactor. (See figure 28)

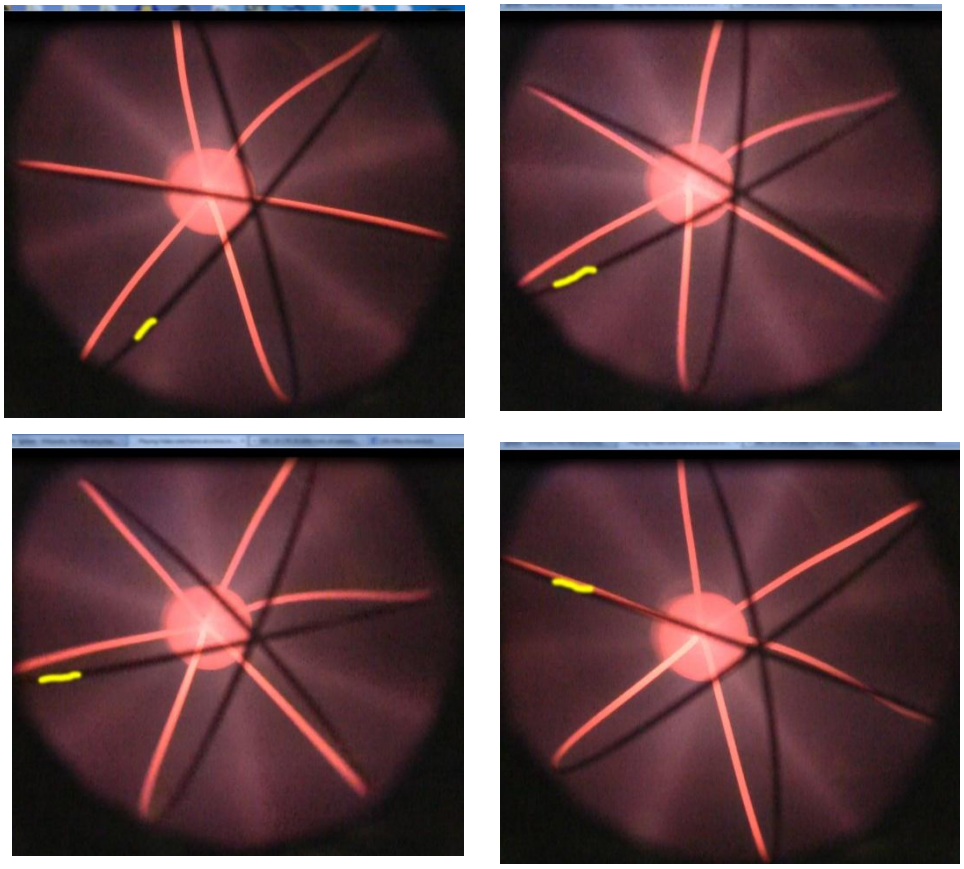

Figure 28 – Starting in time from top left to right, and bottom left to right, video frames of the grid rotation. The yellow marks were added digitally for reference.

b. Analysis of Error

Experiments 1, 2, and 3 were not susceptible to significant error. Observations of plasma were based on visible glowing inside the chamber that cannot be explained by other phenomena. Simple electrical arcing is not a reasonable explanation for what was seen because the size, shape, and varying colors of the glow discharges. The varying colors seen match understood behavior for gases.

Experiment 4 was susceptible to error in voltage measurements that were only accurate to within 500 VDC. The relative ability to control voltage until just the point where plasma was seen was subject to error because plasma initiates at a higher voltage than that required to sustain it. Therefore, over-shoot of the actual voltage at the onset could have occurred. Comparing the curves to known Paschen Discharge Curves was not exact because the effective electrical well distance for this chamber is not known, and the Paschen curve varies with the distance. For this reason, only the general shapes of the plots were relevant as are the general difference between air and deuterium.

Experiment 5 relied on the calibration of the spectrometer, which was accurate to within 0.5 percent. The agreement between the results and National Institute of Standards data for hydrogen reinforces validity of the finding (J. E. Martin). The remaining peaks were not positively identified because of the many known atomic emission lines. A review of spectra for possible gas contaminants like air in-leakage did not show associated atoms like nitrogen and oxygen as matches. It is more likely that the other peaks were associated with atoms of materials used in the chamber like iron, chromium, and tungsten.

Experiment 6 relied on the sensitivity of the Geiger detector. The Geiger detector used was a Ludlum Model 177, which can effectively detect low levels of alpha particles, beta particles, and gamma rays. The silver activation would be

expected to produce beta particles of detectable energies, and therefore, lack of detection is a valid result (Hull, FAQ - Activation Materials - Silver). The lack of silver activation does not prove that fusion was not occurring, but rather only that neutron production rates were not sufficient to produce measurable activation. Future work could repeat this experiment at higher voltages. Experiment 7 measured neutrons with certainty. Error in the magnitude could have been introduced by efficiency and calibration of the Eberline PNC-1 detector. The detector itself is over 40 years old but in good running condition. In the absence of a calibrated neutron source, some error is likely, but given comparison to other IEC devices, the neutron generation rate is reasonable.

E. Conclusions

Based on the results of the experiments, several conclusive statements can be made about the success of the two purposes of the project.

For the first purpose, which was to design and construct an IEC fusion device using commonly available materials to demonstrate the obtainability of fusion with the IEC concept, the following points were demonstrated:

- A vacuum chamber that can be controlled for operation within the left side of the Paschen discharge curve for deuterium fusion fuel was successfully constructed and tested.

- Fusion fuel injection to support control of plasma was demonstrated successfully as indicated by stable plasma over a wide range of voltage and pressure conditions consistent with known IEC fusion.
- The deuterium plasma characteristics including the various glow discharge modes matched known IEC device behavior.
- The deuterium plasma 'star mode' observations indicated that the chamber and inner grid were clean and symmetrical which are prerequisites for efficient IEC operation.
- The IEC device fit easily in the space of a normal workbench. All equipment was obtained and constructed without special methods or permits.

The goal of the second purpose, to build a device that could be used for future research and testing that made use of fusion byproducts such as neutrons, was accomplished. Neutron production levels were easily detected. The device can be used for future neutron studies. The characteristics of the plasma are easily observable as evidenced by the recording of the first documented fusion reactor electromechanical rotation forces.

This project was important because it represents a propagation of IEC fusion research that has yet to realize a full potential of both understanding and practical usage. IEC fusion research has made significant advancements in the last decade especially where practical uses have been developed. The fact that

this project could successfully produce nuclear fusion at the high school level demonstrates how easily fusion can be done though IEC, which is in great contrast to the scale and effort needed to operate and study fusion with other methods.

F. Acknowledgments

The following individuals provided valuable and greatly appreciated assistance:

a. Jay Lyter, Emergency Procedure Programs Manager – Peach Bottom Atomic Power Station, provided advice for the construction and operation of the high voltage power supply.

b. Richard Hull of Richmond Virginia provided advice and encouragement. Mr. Hull is known as the first individual outside of a university or government laboratory environment to achieve deuterium fusion. Mr. Hull graciously demonstrated his own fusion device to this experimenter in October 2011.

c. Carl Willis of Albuquerque, New Mexico provided unusual encouragement and logistical advice for obtaining a supply of deuterium.

d. Bill Fain of Martinsville, Virginia provided encouragement and donation of equipment.

e. Dr. Timothy Koeth of the University of Maryland Physics department provided advice and discounted radiation detection equipment.

f. Patrick Russell of Coral Gables, Florida donated some of the electrical equipment used in the high voltage power supply.

g. The many members of the internet forum Fusors.net provided valuable advice, encouragement, scientific challenge, and a treasure trove of archived operating experience documentation. Several of these individuals also attended the High Energy Amateur Science gathering in Richmond Virginia in October 2011 where important advice and experience was provided. At risk of leaving out some, members who provided direct assistance included Frank Sanns, Doug Coulter, Chris Bradley, Jerry Biehler, Steven Hosemans, and Jon Rosenstiel.

h. Robert Holmes, Radiation Protection Manager – Peach Bottom Atomic Power Station, assisted with efforts to obtain neutron detection equipment for the project.

i. The project mentor contributed numerous hours of advice and safety oversight of the project. The project mentor also financed the majority of the expenses.

G. Bibliography

1. Donovan, David. Spatial Profiling Using a Time of Flight Diagnostic and Applications Deuterium-Deuterium Fusion in Inertial Electrostatic Confinement Fusion Devices. PhD Thesis. Fusion Technology Institute. Madison: University of Wisconsin, 2011.

2. Dupont. "Dupont Viton Flouroelastomer." Dupont Viton Flouroelastomer. Wilmington, Delaware: E.I. du Pont de Nemours and Company, 19 January 2011.

3. Hull, Richard. "FAQ - Activation Materials - Silver." 7 April 2008. The Open Source Fusor Forum. 31 December 2011 <http://www.fusor.net/board/view.php?bn=fusor_neutrons&key=1207603473&pattern=FAQ>.
4. —. "FAQ - Operation of a Fusor." 2011 January 2011. The Open Source Fusor Forum. 31 December 2011 <http://www.fusor.net/board/view.php?bn=fusor_construction&key=1295033886&pattern=FAQ>.
5. —. "FAQ: Fusor Facts and Theory." 11 November 2005. The Open Source Fusor Forum. 31 December 2011 <http://www.fusor.net/board/view.php?bn=fusor_theory&key=1131739884&pattern=FAQ>.
6. Knoll, Glen. Radiation Detection and Measurement. Ann Arbor, Michigan: Wiley & Sons, Inc., 1979.
7. Kulcinski, et. al. "Overview of University of Wisconsin IEC Research Program." 13th U.S. - Japan IEC Workshop. Sydney: University of Wisconsin, 2011. 22.
8. Ligon, Tom. "The World's Simplest Fusion Reactor Revisited or A Not-Quite-So-Simple Fusion Reactor, and How They Made It Work." Analog Science Fiction and Fact (2008): 18.

9. Martin, J. E. Sansonetti and W. C. Handbook of Basic Atomic Spectroscopic Data. Handbook. Gaithersburg, MD: National Institute of Standards and Technology, 2011.

10. Martin, W. C. and Wiese, W. L. Atomic Spectroscopy, A Compendium of Basic Ideas, Notation, Data, and Formulas. Compendium. Gaithersburg, MD: National Institute of Standards and Technology, 2010.

11. Plasma-Universe. Plasma-Universe. 21 August 2008. 31 2008 2011 <http://www.plasma-universe.com/Electric_glow_discharge>.

12. Putterman, Seth. Spontaneous Energy Focusing in Fluid and Solids. Los Angelos: University of California, Los Angelos, 2000.

13. South-Oakleigh, Secondary College Physics. Hydrogen Emission and Absorption Spectrum. 14 August 2010. 31 December 2011 <http://socphysics.blogspot.com/2010/08/hydrogen-emission-and-absorption.html>.

14. Tri-Gas, Matheson. "Deuterium Material Safety Data Sheet." MSDS. Basking Ridge, New Jersey: Matheson Tri-Gas, 12 September 2011.

15. UK, National Physical Laboratory. "4.7 Nuclear Fission and Fusion, and Neutron Interactions." 31 December 2011. Kaye & Laby Tables of Physical & Chemical Constants. 31 December 2011 <http://www.kayelaby.npl.co.uk/atomic_and_nuclear_physics/4_7/4_7_4a.html>.

16. USNRC, United States Nuclear Regulatory Commission. "Energy." 10CFR Code of Federal Regulations. Washington: USNRC, 21 December 2011.

17. Wikipedia. Paschen's Law. 1 December 2011. 31 December 2011 <http://en.wikipedia.org/wiki/Paschen%27s_law>.

18. Willis, Carl. "Activation Measurement Technique." 22 May 2010. The Open Source Fusor Forum. 31 December 2011 <http://www.fusor.net/board/view.php?bn=fusor_neutrons&key=1274513523&pattern=moderator+hdpe>.

H. Attachments

a. Attachment 1 – General Operating Procedure

Purpose:

The purpose of this procedure is to perform the steps to establish and observe deuterium plasma and fusion in the reactor vessel.

1. Verify safety checks are complete.

2. Perform a pre-job brief with all present.

3. Verify system lineup.

    a. Verify vacuum system pre-startup checks are complete
    b. Verify high voltage system pre-startup checks are complete
    c. Verify deuterium delivery system pre-startup checks are complete
    d. Verify neutron detection system pre-startup checks are complete
    e. Verify reactor vessel camera observation system is operating

4. Set the deuterium bottle regulator to approximately 2 psig.

5. Startup the roughing pump and observe improving vacuum on wide range gauge.

6. If the deuterium feed line has been vented, open and then close the needle valve to evacuate the line of air.

7. When reactor pressure drops to less than 0.100 torr start the turbomolecular pump. Allowing pressure to first drop below 0.025 torr is ideal.

8. When vacuum drops below bottom of scale, 0.000 torr, apply power to the ion gauge.

9. Observe continued improving vacuum until reactor pressure is below 6N6 torr. Allowing pressure to drop below 2N6 torr is ideal.

10. Once reactor pressure is at the low target, announce to all present that reactor operations are to commence and verify personnel are clear of high voltage area.

11. If during the remaining steps of the procedure, conditions are unknown or determined unsafe by the test director, shutdown the reactor by turning off the high voltage variac.

12. Turn on the high voltage variac.

13. While observing the reactor camera, grid voltage, and system current, slowly raise grid voltage to approximately 10 kV.

14. Throttle closed the main vacuum valve until pressure starts to rise.

15. Verify open the deuterium regulator outlet valve.

16. Very slightly open the deuterium feed flow control valve and observe reactor pressure and the reactor vessel camera.

17. When pressure indicates 0.001 on the high range pressure indication shutoff the ion gauge.

18. Slowly allow pressure to continue to rise until the chamber atmosphere flashes to plasma.

19. In the next step lower voltage to keep the grid from melting.

20. Adjust the system current to approximately 5 mA using the flow control valve.

21. Raise voltage until current is approximately 10 mA. Make adjustment of the main vacuum valve and needle valve as necessary to keep current between 6 mA and 15 mA. Alternatively lower current and raise voltage until the target voltage is reached.

22. Keep voltage below 25 kV. Verify no detectable x-rays outside the vessel and shielding.

23. Record observations of current, voltage, and pressure at various stable points.

24. Record visual observations of the plasma. Be careful to note color, shape, and density.

25. Record neutron detection data and verify presence of neutrons.

26. To shutdown the reactor, turnoff the variac power, isolate the deuterium supply valves, and open the main vacuum valve.

27. Reduce reactor pressure to below 5N6 torr before shutting off the roughing and turbo pumps.

28. Leaving the chamber isolated and under vacuum is preferred to keep the chamber surfaces free of contaminants.

b. Attachment 2 – Deuterium Light Spectrum Data

Wavelength nm	Relative Intensity	Wavelength nm	Relative Intensity
380.8	0.043461083	418.4	0.042978809
381.7	0.042920992	419.4	0.043272487
382.7	0.043037545	420.3	0.043032038
383.6	0.043682718	421.3	0.043434927
384.6	0.044129659	422.2	0.043040298
385.5	0.043683636	423.2	0.042928333
386.4	0.043344989	424.1	0.043288089
387.4	0.043294513	425	0.043444105
388.3	0.043770821	426	0.04372677
389.3	0.043207327	426.9	0.042983398
390.2	0.043065077	427.9	0.043056817
391.1	0.042794343	428.8	0.04324679
392.1	0.043491828	429.7	0.043610216
393	0.043779081	430.7	0.044107633
394	0.043394547	431.6	0.043580849
394.9	0.043058653	432.6	0.043793765
395.9	0.042794343	433.5	0.043225682
396.8	0.043150427	434.5	0.043508347
397.7	0.043002671	435.4	0.042766811
398.7	0.04286868	436.3	0.042801685
399.6	0.042818204	437.3	0.042744785
400.6	0.042682378	438.2	0.042964125
401.5	0.042487817	439.2	0.043833228
402.4	0.042096859	440.1	0.043589108
403.4	0.04191331	441	0.043746042
404.3	0.042541046	442	0.043524866
405.3	0.04308435	442.9	0.043955288
406.2	0.042935675	443.9	0.044337986
407.2	0.042621807	444.8	0.044008517
408.1	0.042634656	445.8	0.043904812
409	0.043280747	446.7	0.043290842
410	0.043243119	447.6	0.043386287
410.9	0.042916403	448.6	0.04279159
411.9	0.042956783	449.5	0.043166947
412.8	0.043411066	450.5	0.043172453
413.7	0.043676294	451.4	0.043300019
414.7	0.04360471	452.3	0.042929251
415.6	0.04306783	453.3	0.043228435
416.6	0.042748456	454.2	0.043701073
417.5	0.042894377	455.2	0.043822215

Wavelength nm	Relative Intensity	Wavelength nm	Relative Intensity
456.1	0.043422997	495.7	0.043032038
457.1	0.043131155	496.6	0.043414737
458	0.043022861	497.5	0.043233024
458.9	0.042494241	498.5	0.043132072
459.9	0.042408891	499.4	0.04320641
460.8	0.042768646	500.4	0.043310114
461.8	0.043253214	501.3	0.043225682
462.7	0.043352331	502.3	0.043088938
463.6	0.043481732	503.2	0.043319292
464.6	0.043045805	504.1	0.043457871
465.5	0.042623643	505.1	0.043452365
466.5	0.042020686	506	0.043073337
467.4	0.042601617	507	0.043004506
468.4	0.043972725	507.9	0.043003588
469.3	0.044518782	508.8	0.043009095
470.2	0.045032718	509.8	0.042850325
471.2	0.044557327	510.7	0.042724595
472.1	0.04418197	511.7	0.043276158
473.1	0.043766233	512.6	0.043581766
474	0.043422997	513.4	0.043721263
474.9	0.043922249	514.2	0.0433404
475.9	0.043284418	515.1	0.043185301
476.8	0.04354781	515.9	0.043049476
477.8	0.043073337	516.7	0.042809027
478.7	0.043068748	517.6	0.042794343
479.7	0.043174289	518.4	0.043389958
480.6	0.043670787	519.2	0.043294513
481.5	0.044138836	520.1	0.04366161
482.5	0.043629489	520.9	0.043516607
483.4	0.043568	521.8	0.045470481
484.4	0.043268816	522.6	0.04570267
485.3	0.043264227	523.4	0.044745464
486.2	0.043415655	524.3	0.043499169
487.2	0.043631324	525.1	0.042953113
488.1	0.043850665	525.9	0.043907565
489.1	0.042987069	526.8	0.043420244
490	0.042717253	527.6	0.043445023
491	0.04243367	528.4	0.043347742
491.9	0.042837477	529.3	0.043521195
492.8	0.043131155	530.1	0.044066334
493.8	0.042986151	530.9	0.043868102
494.7	0.043013684	531.8	0.043977313

Wavelength nm	Relative Intensity	Wavelength nm	Relative Intensity
533.4	0.043468884	569.3	0.043262392
534.3	0.043025614	570.2	0.043583602
535.1	0.042757633	571	0.043743289
535.9	0.042170278	571.9	0.043655186
536.8	0.042779659	572.7	0.043823133
537.6	0.042777824	573.5	0.043986491
538.5	0.043032038	574.4	0.043745124
539.3	0.042199646	575.2	0.04351936
540.1	0.042641998	576	0.043244037
541	0.042514432	576.9	0.042825546
541.8	0.043242201	577.7	0.043121977
542.6	0.042992575	578.5	0.042607124
543.5	0.0430559	579.4	0.042930169
544.3	0.042742949	580.2	0.042505254
545.1	0.043146756	581	0.042806274
546	0.04341749	581.9	0.043476226
546.8	0.043855254	582.7	0.043486321
547.6	0.0437956	583.5	0.043891963
548.5	0.043829557	584.4	0.043033874
549.3	0.043757055	585.2	0.042889788
550.1	0.04384057	586	0.042857667
551	0.043819462	586.9	0.042965961
551.8	0.044081018	587.7	0.042976056
552.6	0.04451144	588.5	0.043022861
553.5	0.044855593	589.3	0.043075172
554.3	0.044692235	590	0.043493663
555.2	0.043943357	590.8	0.043817626
556	0.0438525	591.5	0.044081936
556.8	0.043194479	592.3	0.043621229
557.7	0.043336729	593	0.043180713
558.5	0.043106376	593.8	0.043154098
559.3	0.043534044	594.5	0.043064159
560.2	0.043420244	595.3	0.043286253
561	0.043174289	596.1	0.043315621
561.8	0.043245872	596.8	0.043403724
562.7	0.043375274	597.6	0.043281664
563.5	0.043324798	598.3	0.04327524
564.3	0.042945771	599.1	0.043912154
565.2	0.043152263	599.8	0.044242541
566	0.043025614	600.6	0.044055322
566.8	0.043313785	601.3	0.043301855
567.7	0.042889788	602.1	0.042549306

Wavelength nm	Relative Intensity	Wavelength nm	Relative Intensity
603.6	0.043126566	635.3	0.043969971
604.4	0.043193561	636	0.043768986
605.1	0.042765893	636.8	0.043834146
605.9	0.042965043	637.6	0.043499169
606.6	0.043177959	638.3	0.043632242
607.4	0.043489992	639.1	0.042929251
608.1	0.043846076	639.8	0.042402467
608.9	0.043687307	640.6	0.042870516
609.6	0.043343153	641.3	0.042787001
610.4	0.042973303	642.1	0.043389958
611.1	0.043089856	642.8	0.042687885
611.9	0.043525784	643.6	0.043144921
612.7	0.044099373	644.3	0.043163276
613.4	0.044083772	645.1	0.043638666
614.2	0.043816708	645.9	0.043472555
614.9	0.043464295	646.6	0.043411066
615.7	0.043674458	647.4	0.043512936
616.4	0.04364142	648.1	0.043279829
617.2	0.043853418	648.9	0.043347742
617.9	0.043383534	649.6	0.043062324
618.7	0.043579013	650.4	0.044007599
619.4	0.043533126	651.1	0.044131494
620.2	0.044175546	651.9	0.044468306
621	0.043972725	652.6	0.044244377
621.7	0.043648762	653.4	0.043920413
622.5	0.043505594	654.2	0.044023201
623.2	0.044156273	654.9	0.045152024
624	0.04458853	655.7	0.046714022
624.7	0.044174628	656.4	0.047909841
625.5	0.044081936	657.2	0.046798455
626.2	0.043589108	657.9	0.045265824
627	0.043621229	658.7	0.043888292
627.7	0.043103622	659.4	0.043469802
628.5	0.043127484	660.2	0.043890128
629.3	0.043762562	660.9	0.044269156
630	0.043987409	661.7	0.044179217
630.8	0.044069088	662.5	0.044283839
631.5	0.04371025	663.2	0.043779081
632.3	0.043646926	664	0.043978231
633	0.043582684	664.7	0.043407395
633.8	0.043393629	665.5	0.043382616
634.5	0.043521195	666.2	0.043543221

Wavelength nm	Relative Intensity	Wavelength nm	Relative Intensity
667	0.044337069	698.8	0.044411406
667.8	0.044760148	699.6	0.044026872
668.5	0.04473078	700.3	0.044251718
669.3	0.044087443	701.1	0.043668952
670	0.043821297	701.8	0.043389958
670.8	0.043768986	702.6	0.042788837
671.5	0.043512936	703.3	0.043183466
672.3	0.043232106	704.1	0.042987069
673.1	0.043534044	704.9	0.043694649
673.8	0.043788258	705.6	0.043644173
674.6	0.044080101	706.4	0.044038802
675.3	0.043816708	707.1	0.043379863
676.1	0.043818544	707.9	0.043788258
676.8	0.044029625	708.6	0.04369006
677.6	0.044226022	709.4	0.043987409
678.4	0.044443527	710.1	0.043456036
679.1	0.043980067	710.9	0.043971807
679.9	0.043372521	711.6	0.043713921
680.6	0.042698898	712.4	0.044130576
681.4	0.042923745	713.1	0.043871773
682.1	0.04313299	713.9	0.044112222
682.9	0.043571671	714.6	0.044147096
683.7	0.04408836	715.4	0.043526702
684.4	0.044510522	716.1	0.043709333
685.2	0.044984995	716.9	0.043479897
685.9	0.044500427	717.6	0.0439094
686.7	0.044382956	718.4	0.043890128
687.4	0.043512936	719.1	0.043577178
688.2	0.043551481	719.8	0.043585437
689	0.043428503	720.6	0.043116471
689.7	0.043769904	721.3	0.043384452
690.5	0.043918578	722.1	0.043123813
691.2	0.043842405	722.8	0.043811202
692	0.044154438	723.6	0.043779081
692.7	0.044199407	724.3	0.043945192
693.5	0.044918917	725.1	0.043829557
694.3	0.044612391	725.8	0.043805696
695	0.044506851	726.6	0.043577178
695.8	0.044009434	727.3	0.043365179
696.5	0.044100291	728.1	0.04338904
697.3	0.044504098	728.8	0.043862596
698	0.044336151	729.6	0.043649679

Wavelength nm	Relative Intensity	Wavelength nm	Relative Intensity
730.3	0.043642337	761.8	0.043678129
731.1	0.043430339	762.5	0.044752806
731.8	0.044304948	763.3	0.045051072
732.6	0.04409662	764	0.044565586
733.3	0.043940604	764.8	0.044326056
734.1	0.043210998	765.5	0.04399108
734.8	0.043376192	766.2	0.044514193
735.6	0.043620311	767	0.044701412
736.3	0.043922249	767.7	0.04519424
737.1	0.04406817	768.5	0.044988666
737.8	0.044282004	769.2	0.044788598
738.6	0.043900223	770	0.044442609
739.3	0.043848829	770.7	0.044876701
740.1	0.043390876	771.5	0.045156613
740.8	0.043175206	772.2	0.045315382
741.6	0.043233024	773	0.044886796
742.3	0.044178299	773.7	0.044823472
743	0.044884961	774.5	0.044998761
743.8	0.044859264	775.2	0.044783092
744.5	0.044235199	776	0.044669291
745.3	0.043366097	776.7	0.044579353
746	0.043196314	777.5	0.044319631
746.8	0.042777824	778.2	0.04443802
747.5	0.043171535	779	0.044402228
748.3	0.043152263	779.7	0.044959298
749	0.043242201	780.5	0.045171297
749.8	0.04355974	781.2	0.045217184
750.5	0.043995668	782	0.044963887
751.3	0.044062663	782.7	0.044226939
752	0.044023201	783.5	0.044112222
752.8	0.043979149	784.2	0.044163615
753.5	0.044296688	785	0.045065756
754.3	0.044416912	785.7	0.045184145
755	0.044296688	786.5	0.045226361
755.8	0.044322385	787.2	0.044982242
756.5	0.04407643	788	0.044769325
757.3	0.044428843	788.7	0.044725274
758	0.043913989	789.4	0.04445454
758.8	0.044346246	790.2	0.04408836
759.5	0.044196654	790.9	0.04413333
760.3	0.043770821	791.7	0.043955288
761	0.043444105	792.4	0.044033296

Wavelength nm	Relative Intensity	Wavelength nm	Relative Intensity
793.2	0.044094784	824.6	0.04421868
793.9	0.043757055	825.4	0.043679965
794.7	0.044099373	826.1	0.043717592
795.4	0.04459679	826.9	0.043855254
796.2	0.04466562	827.6	0.043956205
796.9	0.044795022	828.4	0.044602296
797.7	0.043994751	829.1	0.04475923
798.4	0.044192065	829.9	0.04478768
799.2	0.04416178	830.6	0.04449492
799.9	0.04459679	831.4	0.044168204
800.7	0.045044648	832.2	0.043790094
801.4	0.045475987	833	0.043500087
802.2	0.044524288	833.8	0.043222011
802.9	0.044896892	834.6	0.043488157
803.7	0.044632582	835.4	0.043252297
804.4	0.045070345	836.3	0.043512018
805.2	0.044078265	837.1	0.04346246
805.9	0.043646926	837.9	0.04376715
806.7	0.043802025	838.7	0.044150767
807.4	0.044347164	839.5	0.044707837
808.2	0.044465553	840.4	0.044931766
808.9	0.044552738	841.2	0.044721603
809.7	0.044609638	842	0.044359094
810.4	0.044472894	842.8	0.044543561
811.2	0.044714261	843.6	0.044158109
811.9	0.044556409	844.5	0.04413333
812.6	0.044241623	845.3	0.044355423
813.4	0.044382956	846.1	0.044723438
814.1	0.044134247	846.9	0.044951956
814.9	0.044282004	847.8	0.043910318
815.6	0.044030542	848.6	0.043835981
816.4	0.04403972	849.4	0.043349577
817.1	0.044259978	850.2	0.043638666
817.9	0.043925002	851	0.043399135
818.6	0.044634417	851.9	0.044171875
819.4	0.044642677	852.7	0.044377449
820.1	0.044841827	853.5	0.044814295
820.9	0.044081018	854.3	0.044626158
821.6	0.043960794	855.1	0.044738122
822.4	0.044193901	856	0.044268238
823.1	0.044757395	856.8	0.043658857
823.9	0.044400393	857.6	0.043249543

Wavelength nm	Relative Intensity	Wavelength nm	Relative Intensity
858.4	0.043233024	892.9	0.044188394
859.2	0.043235777	893.7	0.043299102
860.1	0.043634995	894.6	0.042459367
860.9	0.043385369	895.4	0.042166607
861.7	0.043510182	896.2	0.042531869
862.5	0.043640502	897	0.042690638
863.4	0.043906647	897.8	0.042530033
864.2	0.043827721	898.7	0.042716335
865	0.04366987	899.5	0.043600121
865.8	0.043724934		
866.6	0.043825886		
867.5	0.043623982		
868.3	0.043196314		
869.1	0.04342575		
869.9	0.043388123		
870.7	0.043453282		
871.6	0.042879693		
872.4	0.042683296		
873.2	0.042871433		
874	0.042790672		
874.9	0.042693391		
875.7	0.042673201		
876.5	0.042987069		
877.3	0.043407395		
878.1	0.043548728		
879	0.043372521		
879.8	0.043700155		
880.6	0.043311032		
881.4	0.043187137		
882.2	0.042733772		
883.1	0.043273405		
883.9	0.043333058		
884.7	0.043035709		
885.5	0.042931087		
886.3	0.043186219		
887.2	0.0437956		
888	0.043656103		
888.8	0.043965383		
889.6	0.043367014		
890.5	0.043753384		
891.3	0.043587273		
892.1	0.04423061		